CHAPTER IV
RESULTS AND DISCUSSION

4.1 Effect of natural rubber's mastication time on the melt flow index and tensile properties of PLA/NR blends

4.1.1 Melt flow index (MFI)

The melt flow index (MFI) is an essential indicator in polymer processing that assesses the flow properties of thermoplastic polymers. It indirectly indicates the molecular weight and viscosity of the melt, providing important information about the processing abilities of these materials. As the MFI increases, the viscosity and molecular weight decrease. (Chaiwutthinan, Chuayjuljit, Srasomsub, and Boonmahitthisud, 2019). Figure 4.1 shows the MFI values of the neat PLA and PLA/NR blends at various mastication times of NR, including 10, 20, and 30 min. The melt flow index (MFI) of the PLA/NR blends was higher than that of neat PLA and showed an increase with the NR's mastication time.

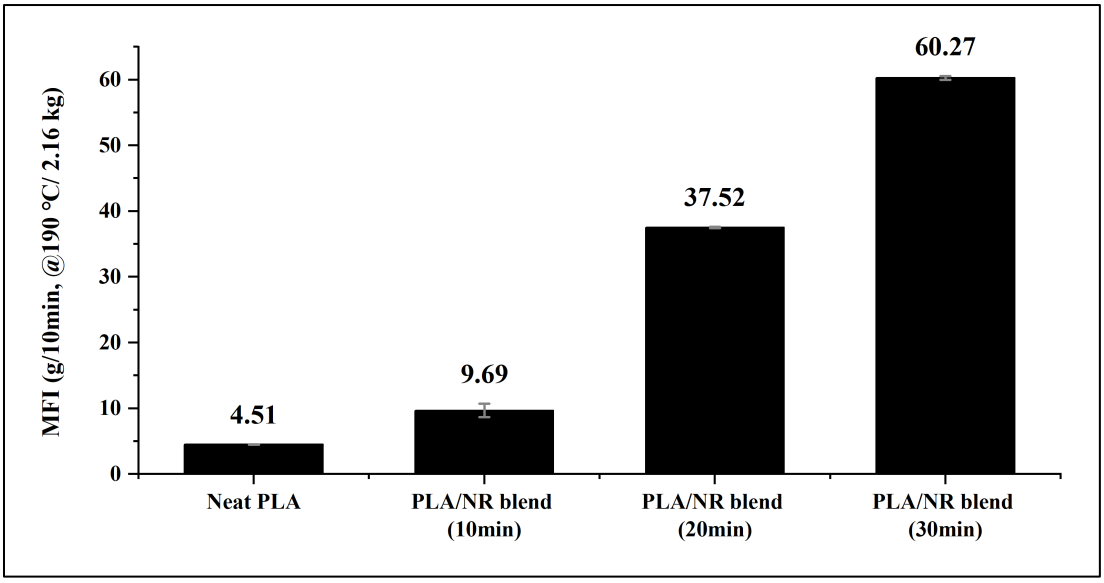

Figure 4.1 Melt flow index (MFI) of neat PLA and its blends with masticated NR at different mastication times.

The results that were observed correspond to the presence of NR, which acts as an attribute of a plasticizer and enhances the chain mobility of PLA (Tessanan, Chanthateyanonth, Yamaguchi, and Phinyocheep, 2020). Additionally, a decrease in viscosity occurred because of long mastication time (Phattarateera and Pattamaprom, 2019).

4.1.2 Tensile properties

Tensile stress-strain curves for neat PLA and PLA/NR blends at various mastication times of NR are shown in Figure 4.2. The addition of NR to the PLA matrix transformed the PLA's brittle fracture characteristics into ductile fracture behavior. Table 4.1 shows the summary of the tensile strength, Young's modulus, and elongation at break of the neat PLA and PLA/NR blends.

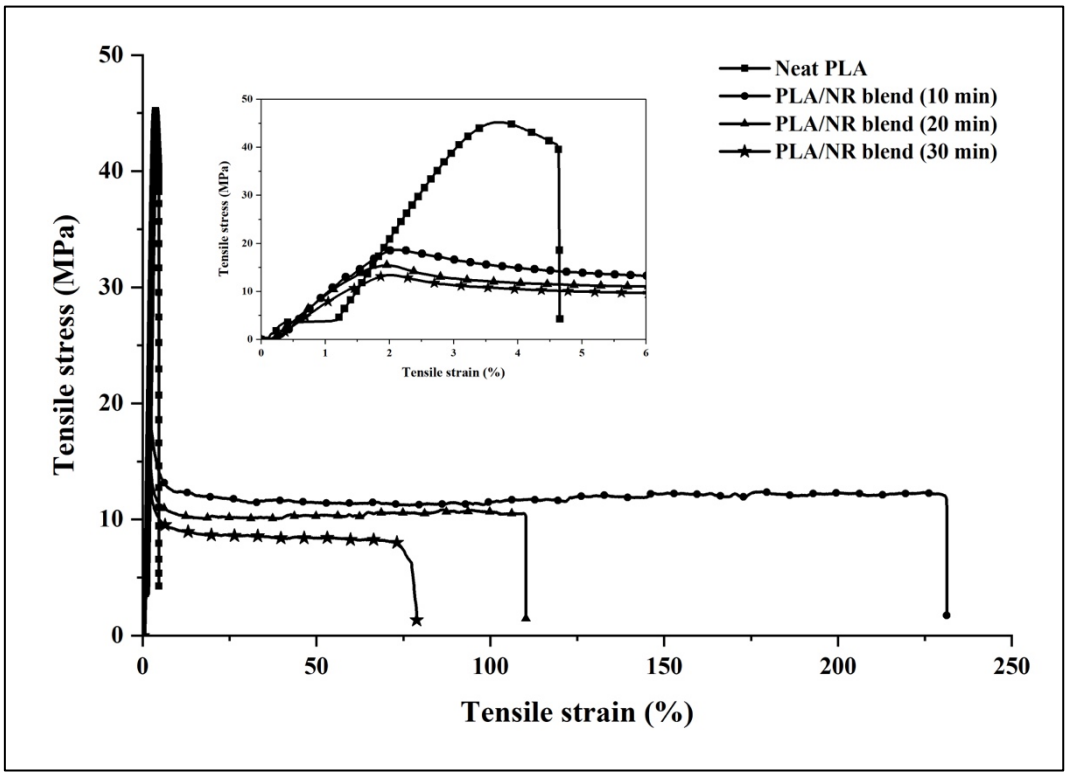

Figure 4.2 Stress-strain curves of neat PLA and its blends with masticated NR at different mastication times.

The tensile properties of neat PLA and the blends of PLA and masticated NR at various mastication times are compared in Figure 4.3 (a-c). The addition of NR into the PLA matrix resulted in a decrease in both tensile strength and

modulus. The decrease in both properties was more significant with an increase in the mastication time of NR. Due to its elastic properties that help lessen PLA's brittleness, NR's rubbery nature causes a decrease in the blends' tensile strength and modulus (Buys et al., 2017). Bitinis et al. (2011), Pongtanayut et al. (2013), and Xu et al. (2014) have all discovered similar tendencies.

The addition of NR enhanced the elongation at break of PLA. The flexibility and softness of natural rubber (NR) would enhance the elongation of the blend. The mastication of NR could decrease its molecular weight, improving the interfacial adhesion between PLA and NR, which leads to improved compatibility with PLA. However, throughout the process of mastication, when the time was extended to 20 and 30 minutes, it was seen that there was a significant decrease in the elongation at break. At overly long masticating time resulted in a reduction in viscosity. The decreased viscosity of the rubber led to the formation of a combined rubber particle, which is a low-entanglement network that caused a decrease in elongation at break, but it remained greater than that of PLA (Jaratrotkamjorn et al., 2012; Phattarateera and Pattamaprom, 2019). Therefore, if the objective is to enhance the toughness of PLA, a 10-minute mastication time for NR seems to be the most appropriate choice for continued study.

Table 4.1 Summary of tensile properties of neat PLA and its blends with masticated NR at different mastication times.

Sample	**Tensile strength (MPa)**	**Young's Modulus (GPa)**	**Elongation at break (%)**
Neat PLA	45.21 ± 1.03	2.11 ± 0.63	4.66 ± 1.15
PLA/NR blend (10min)	18.66 ± 0.36	1.27 ± 0.28	231.33 ± 34.43
PLA/NR blend (20min)	15.46 ± 0.17	1.02 ± 0.12	110.26 ±14.23
PLA/NR blend (30min)	13.40 ± 0.19	0.85 ± 0.03	78.84 ± 5.41

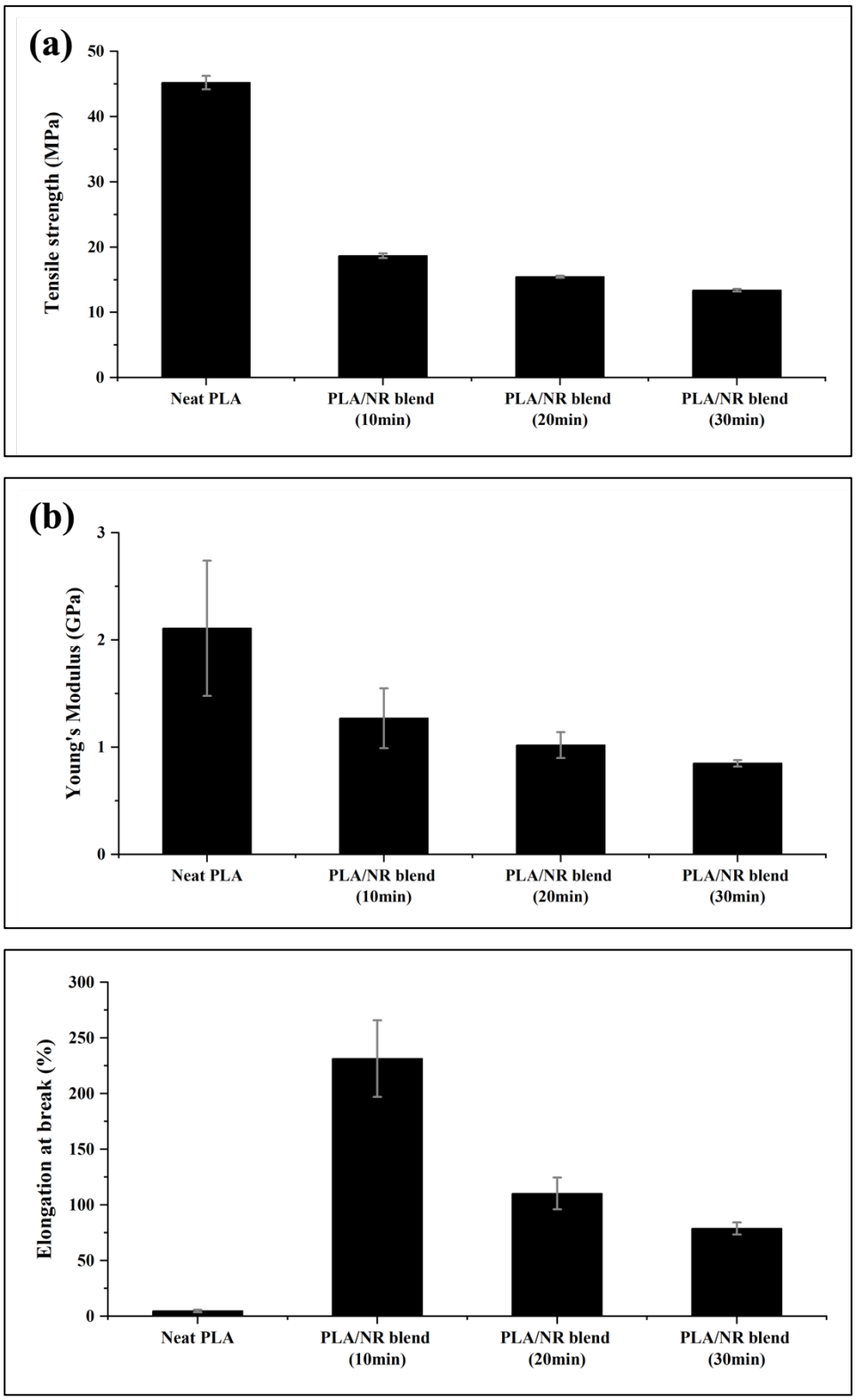

Figure 4.3 Tensile properties of neat PLA and its blends with masticated NR at different mastication times: Tensile strength (a), Young's Modulus (b), and Elongation at break (c).

4.2 Effect of an amount of rice straw on melt flow index, tensile properties, and morphological characteristics of PLA/NR/RS biocomposite films

This study intends to create environmentally friendly and biodegradable biocomposites using renewable and biodegradable materials, which include PLA, NR, and rice straw (RS). After determining the most effective mastication time for NR to be mixed with PLA, the 10-minute masticated NR was chosen to be blended with PLA at a constant ratio of 60% PLA and 40% NR by weight. The PLA/NR blend matrix was then filled with RS at weight percentages of 3%, 5%, and 10%. The RS fiber was expected to decrease the cost of biocomposites without compromising their mechanical properties while simultaneously enhancing their biodegradability. Subsequently, the effect of RS content on the melt flow index (MFI), tensile properties, and morphological properties of the bicomposite films were investigated.

4.2.1 Physical characteristics

Figure 4.4 (a-e) shows the physical characteristics of neat PLA, PLA/NR blend, and PLA/NR/RS biocomposite films. All biocomposite films exhibited an opaque light brown tint, while neat PLA film was slightly yellow and transparent, and PLA/NR blend film was semi-opaque. The surface appearance of the neat PLA, PLA/NR blend, PLA/NR/3%RS, and PLA/NR/5%RS films was smooth. The surface of the PLA/NR/10 % RS film, on the other hand, contained numerous huge holes; hence, this film had not been subjected to further characterization. The PLA films were 0.20 ± 0.01 mm thick. The thickness of the films decreased to 0.05 ± 0.01 mm with the addition of NR.

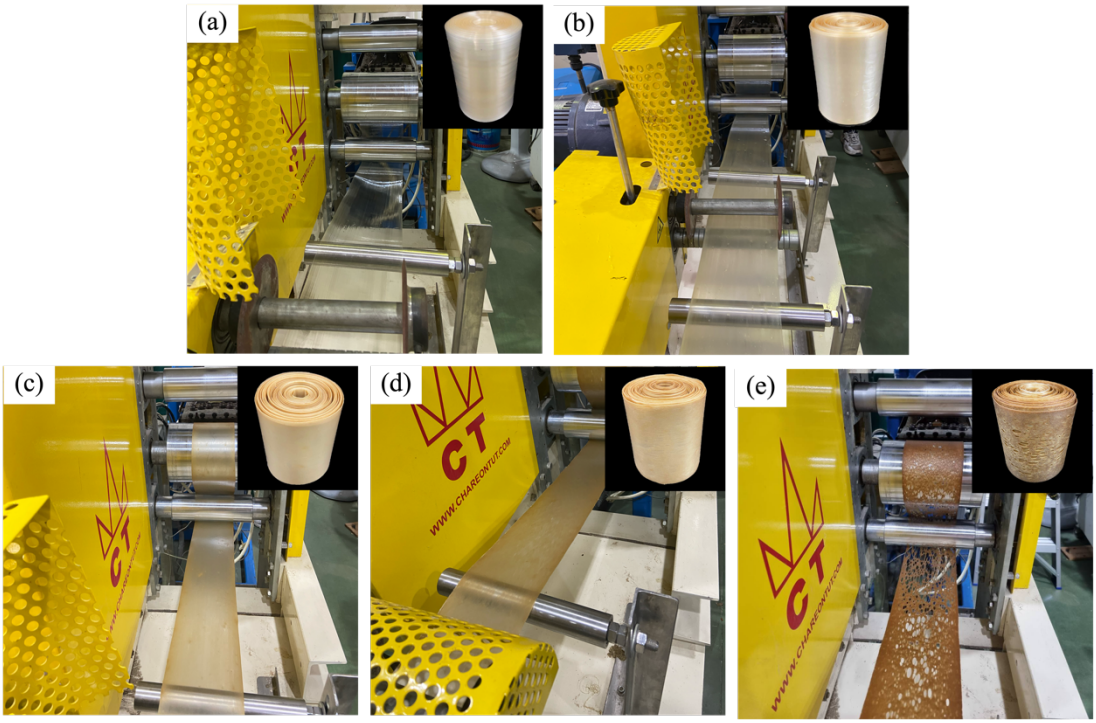

Figure 4.4 Physical characteristics of neat PLA (a), PLA/NR blend (b), and PLA/NR/RS biocomposite films; 3 wt.% (c), 5 wt.% (d), and 10 wt.% RS (e).

This might be because NR improved the melt strength of PLA/NR film, thus facilitating stretchability (Zhao et al., 2023). The thickness of the biocomposite films was 0.14 ± 0.01, 0.16 ± 0.01, and 0.24 ± 0.01 mm for the films at 3, 5, and 10 %wt. RS, respectively. Table 4.2 shows the thickness and width from extrusion process of the neat PLA and PLA/NR blend and PLA/NR/RS biocomposite films at 3, 5, and 10 wt.% RS. The thickness of the biocomposite films tended to increase with an increase in RS content, which was consistent with the increase in melt flow rate.

Table 4.2 The thickness and width of the neat PLA and PLA/NR blend and PLA/NR/RS biocomposite films.

Sample	Thickness (mm)	Width (mm)
Neat PLA	0.20 ± 0.01	123.98 ± 0.02
PLA/NR blend	0.05 ± 0.01	109.02 ± 0.01
PLA/NR/3%RS	0.14 ± 0.01	103.23 ± 0.02
PLA/NR/5%RS	0.16 ± 0.01	104.14 ± 0.02
PLA/NR/10%RS	0.24 ± 0.01	116.27 ± 0.07

4.2.2 Melt flow index (MFI)

Figure 4.5 shows the MFI values of neat PLA, PLA/NR blend, and all PLA/NR/RS biocomposites. The PLA/NR blend had a higher MFI than neat PLA. The addition of 40 %wt. NR improves the melt flow properties of neat PLA because it acts as an attribute of a plasticizer and enhances the chain mobility of PLA, as mentioned above in Topic 4.1.1. The MFI values of the composites containing 3 and 5 %wt. RS were similar and approximately twice that of PLA/NR. The higher the amount of fiber added during composite manufacturing causes an increase in shear (Eselini, Tirkes, Akar, and Tayfun, 2019). When RS content was increased to 10 %wt., the MFI increased to around 37±0.79 g/10 min, which could not be used to produce a smooth film. In general, the range of MFI that is suitable for cast film is around 9-15 g/10 min, which makes the cast film extrusion process smoother (Van Krevelen and Te Nijenhuis, 2009). The large and numerous holes were then occurred in the films at 10 %wt. RS.

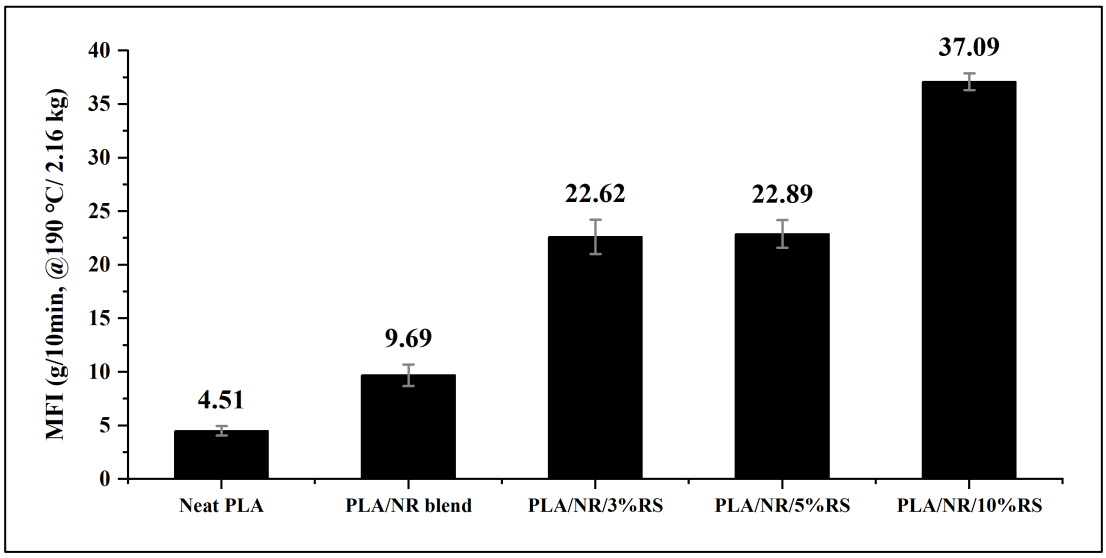

Figure 4.5 Melt flow index (MFI) of neat PLA, PLA/NR blend, and PLA/NR/RS biocomposites.

4.2.3 Tensile properties

Tensile stress-strain curves of neat PLA, PLA/NR, and PLA/NR/RS biocomposites are shown in Figure 4.6 (a-b). The neat PLA showed brittle fractures. The natural brittleness of neat PLA transformed into a more ductile fracture when NR

was added. At the RS contents of 3–5 %wt., the fracture behavior of the films was still ductile.

The tensile properties of neat PLA, PLA/NR, and PLA/NR/RS biocomposite films in machine (MD) and transverse direction (TD) are compared in Figure 4.7 (a-c). In addition, a comparison is performed with the characteristics of HDPE to evaluate its features for use as an agricultural film.

In MD, PLA/NR blend and PLA/NR/RS biocomposites films showed lower tensile strength and modulus values (Figure 4 (a-b)) than neat PLA. The rubbery nature of NR leads to a decrease in tensile strength and modulus. Also, the tensile strength and modulus of PLA/NR/RS biocomposites films were lower compared to neat PLA and PLA/NR blends, and they decreased with increasing RS contents. This is common in natural fiber composites. The PLA are hydrophobic, but the most natural fibers are hydrophilic, which prevents them from forming good interfacial adhesion (Alias, Ismail, and Ishak, 2021). The tensile strength and modulus of the films are lower in the transverse direction (TD) than they are in the machine direction, but both directions exhibit the same trend.

Elongation at break of neat PLA, PLA/NR, and PLA/NR/RS biocomposite films is shown in figure 4 (c). When RS is added, the elongation at break of PLA/NR/RS biocomposite films is decreased. As a result of poor interfacial adhesion. Moreover, the presence of RS fiber limits the mobility of PLA and NR polymeric chains, which hinders the chains' ability to rearrangement (Yaisun and Trongsatitkul, 2023). As a result, elongation at break decreases. However, all biocomposite films still showed a significantly higher elongation at break than that neat PLA. The films' elongation at break is much lower in the transverse direction than it is in the machine direction.

The neat PLA, PLA/NR blend, and PLA/NR/RS biocomposite films exhibit better tensile strength and modulus characteristics compared to HDPE. While the elongation at break of all films was less than HDPE, indicating their lower elasticity, both the PLA/NR blend and PLA/NR/RS biocomposite films were able to produce film. Table 4.3 shows the summary of the tensile strength, Young's modulus, and elongation at break of the HDPE, neat PLA, PLA/NR blend, and PLA/NR/RS biocomposite films.

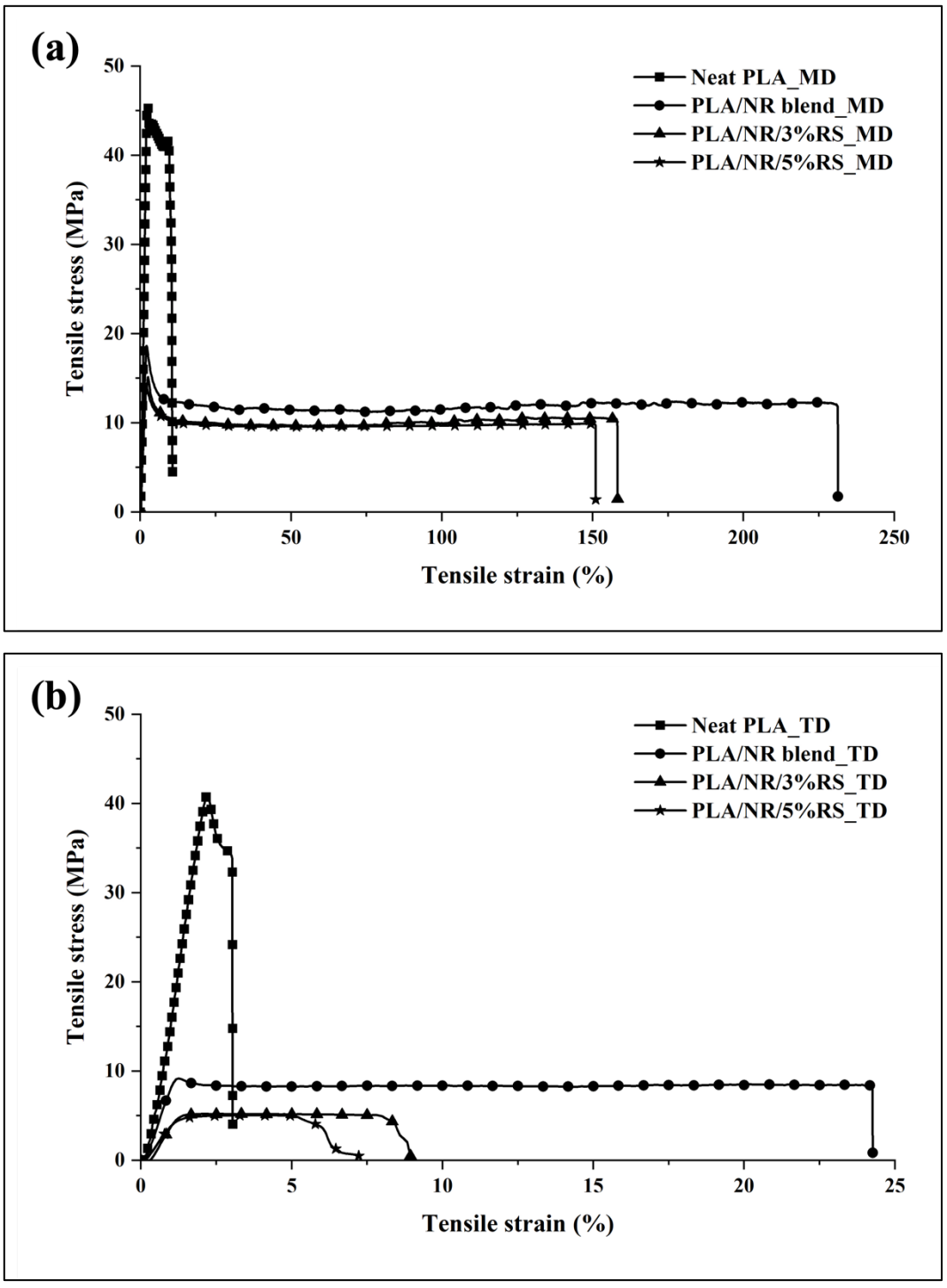

Figure 4.6 Stress-strain curve of neat PLA, PLA/NR, and PLA/NR/RS biocomposite films; machine direction (MD) (a) and transverse direction (TD) (b).

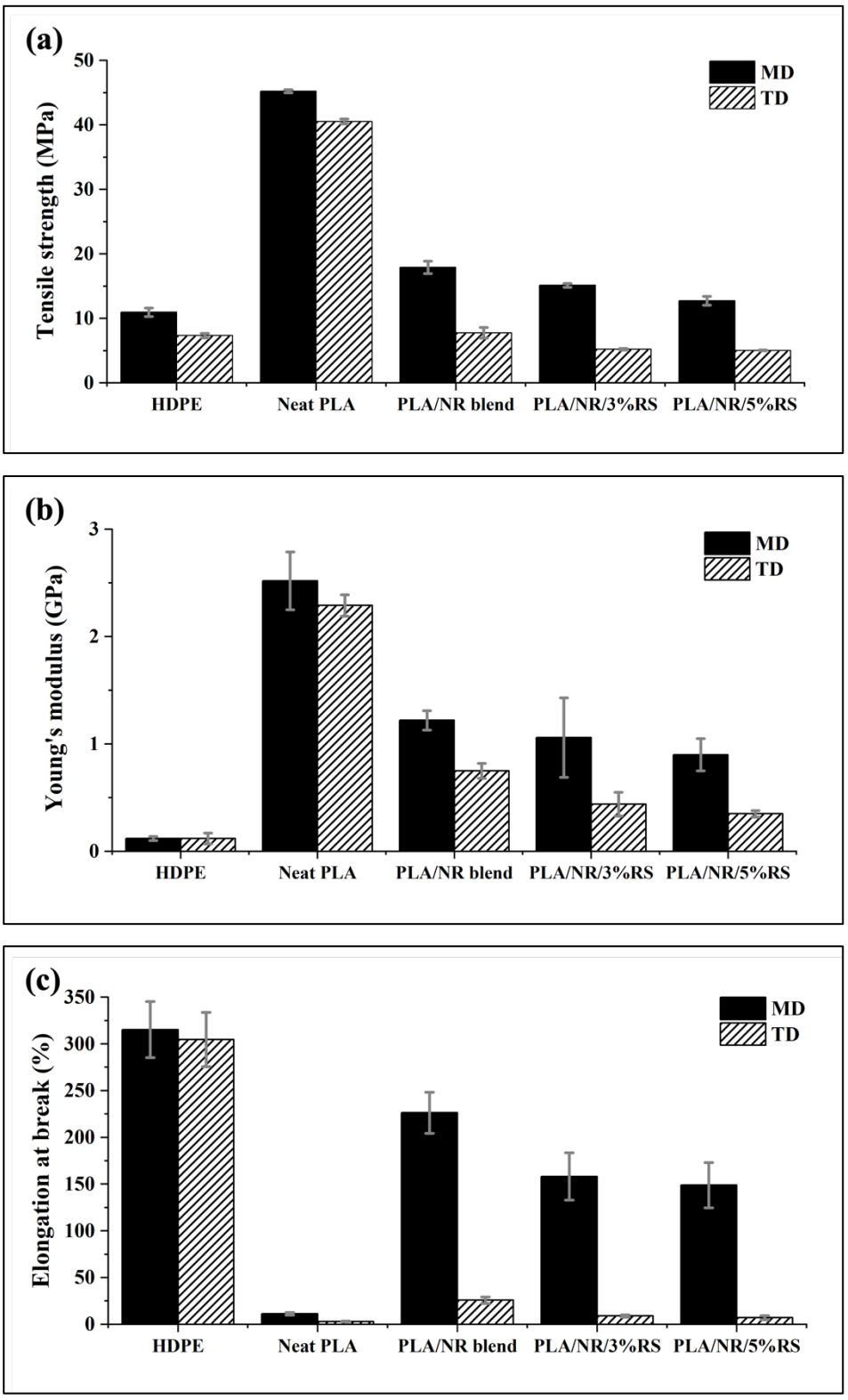

Figure 4.7 Tensile properties of HDPE, neat PLA, PLA/NR blend, and PLA/NR/RS biocomposites films; Tensile strength (a), Young's Modulus (b), and Elongation at break (c)

Table 4.3 Summary of tensile properties of HDPE, neat PLA, PLA/NR blend, and PLA/NR/RS biocomposite films.

Sample		Tensile Strength (MPa)	Young's Modulus (GPa)	Elongation at break (%)
HDPE	MD	11.86 ± 0.66	0.12 ± 0.02	314.93 ± 35.49
	TD	11.29 ± 0.36	0.12 ± 0.05	307.43 ± 35.15
Neat PLA	MD	45.22 ± 0.25	2.52 ± 0.27	11.26 ± 1.38
	TD	40.55 ± 0.38	2.29 ± 0.10	3.10 ± 0.34
PLA/NR blend	MD	19.11 ± 0.98	1.22 ± 0.09	226.31 ± 28.43
	TD	10.58 ± 0.85	0.75 ± 0.07	25.86 ± 3.46
PLA/NR/3%RS	MD	15.14 ± 0.30	1.06 ± 0.37	158.24 ± 25.30
	TD	5.22 ± 0.12	0.44 ± 0.11	8.94 ± 1.36
PLA/NR/5%RS	MD	14.38 ± 0.62	0.90 ± 0.15	148.90 ± 24.12
	TD	5.04 ± 0.06	0.35 ± 0.03	7.21 ± 2.22

4.2.4 Morphological properties

Figure 4.8 (a–d) shows the FE-SEM micrographs of the tensile fractured surfaces of neat PLA, PLA/NR blend, and PLA/NR/RS biocomposite films. The surface of the neat PLA film was smooth, which is typical for brittle polymers. Phase separated morphology could be seen in the PLA/NR blends, many NR droplets were found in the PLA matrix. This indicated that blends of PLA and NR were immiscible. When RS fibers were added to PLA/NR, it was discovered that the lager extent of phase separation. This occurs from the difference in polarity of the composite system. Only a little amount of the RS fiber could be observed on the fracture surface of PLA/NR/RS biocomposite films. It shows that the RS fiber was well embedded in the polymer matrix.

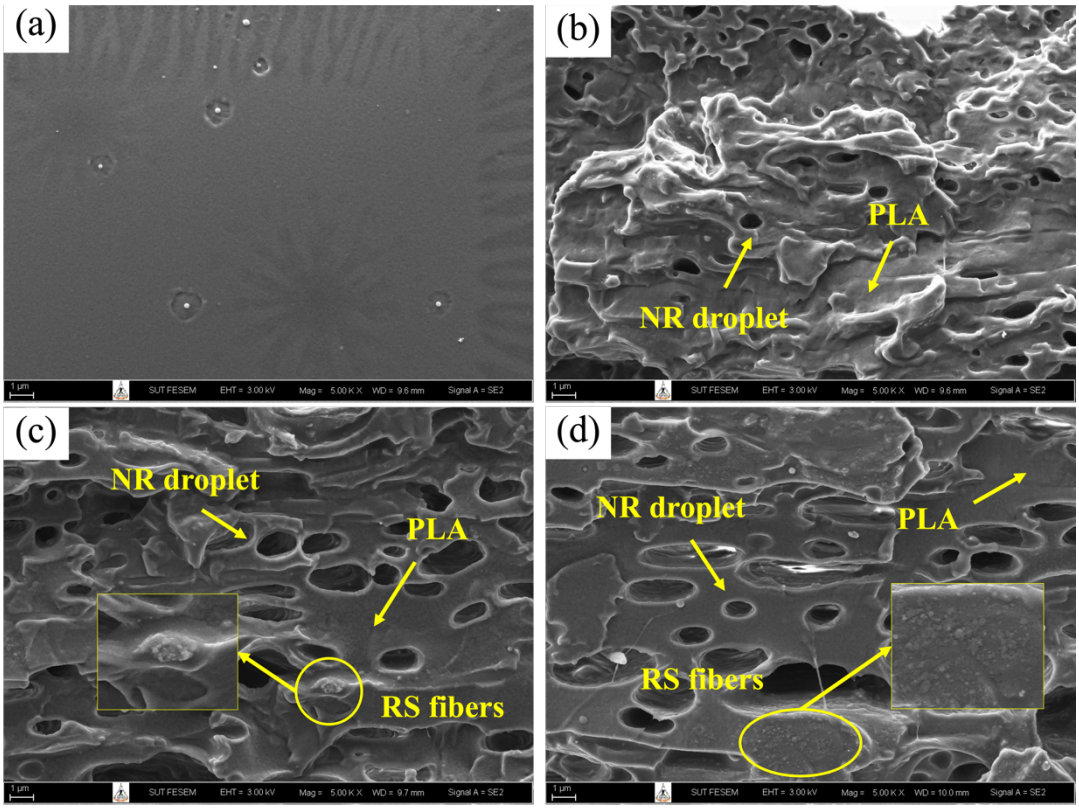

Figure 4.8 FE-SEM micrographs at 5000x magnification of tensile fracture surface of neat PLA (a) PLA/NR blend (b), and PLA/NR/RS biocomposite films with RS concentrations of 3 wt.% (c) and 5 wt.% (d).

4.3 Soil burial degradation of PLA/NR/RS biocomposite films

4.3.1 Physical appearance

The degradation of neat PLA, PLA/NR blend, and PLA/NR/RS biocomposites was confirmed by visually observing the physical appearance of the samples. Figure 4.9 shows the appearance of film samples before and after the burial test. After being buried in soil for a period of 90 days, the previously clear, neat PLA became opaque and turned white. The PLA/NR blend and PLA/NR/RS biocomposite exhibited a little alteration in colour, and the presence of fungi was noticeably observed on the surface.

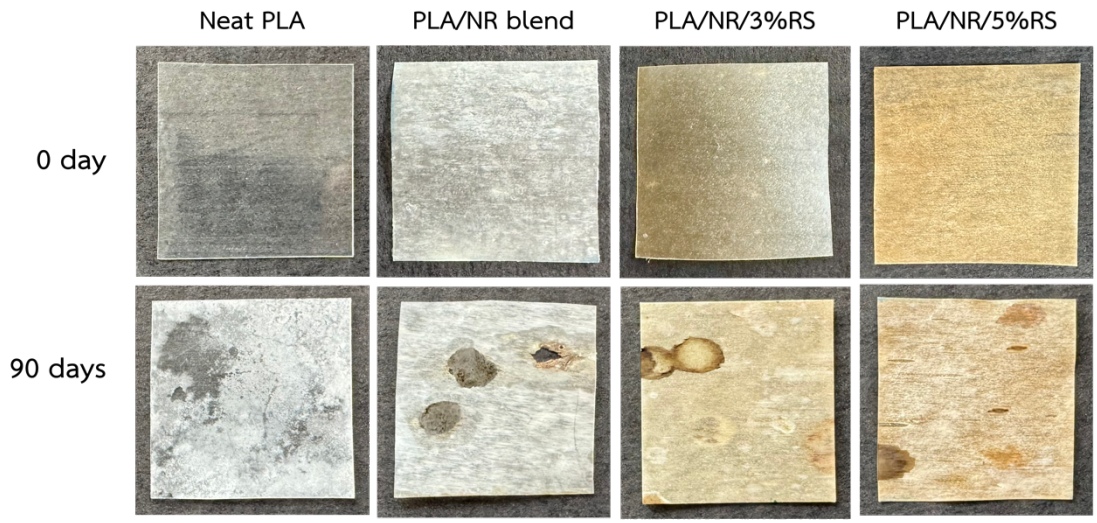

Figure 4.9 Physical appearance of the films before and after soil burial test for 90 days.

4.3.2 Biodegradability

4.3.2.1 Weight loss percentage

The film samples' weight loss percentages, following burial in soil for various durations (15, 30, 60, and 90 days), are graphically represented in Figure 4.10. The study findings indicate that neat PLA demonstrates the lowest percentage of weight loss. This suggests a comparatively slower degradation rate when compared to both the PLA/NR blend and the PLA/NR/RS biocomposite. PLA breakdown occurs primarily through hydrolytic and microbial processes, which are accelerated by high temperatures, humidity, and water absorption (Matta, Rao, Suman, and Rambabu, 2014; Fabian et al., 2023). The study suggests that the soil temperature and moisture conditions may not reach the optimal conditions required to facilitate the decomposition of PLA. According to additional reports, if the temperature remains below the Tg, the deterioration of the PLA is confined to its surface (Elsawy et al., 2017; Karamanlioglu and Alkan, 2019).

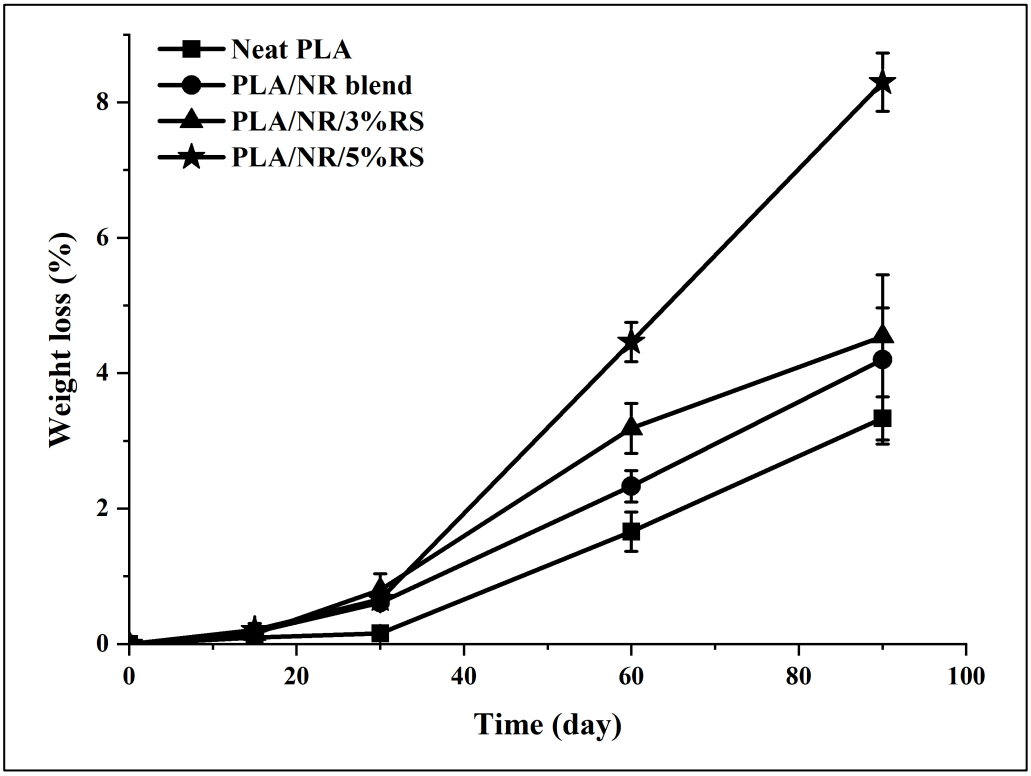

Figure 4.10 Weight loss percentage of neat PLA, PLA/NR blend, and PLA/NR/RS biocomposite films after being buried in soil for 90 days.

The incorporation of the NR and PLA resulted in an increase in the weight loss percentage. This is the result of the incompatibility between PLA and NR. Structures composed of heterogeneous materials typically undergo faster destruction than those composed of homogeneous ones (Tertyshnaya et al., 2022). The heterogeneous structure of the PLA/NR blend causes an increased percentage of water absorption (Huang et al., 2013; Rosli et al., 2018). NR increases the efficiency of water absorption, which is the primary mechanism for PLA degradation and involves hydrolysis. This phenomenon leads to an augmentation in the crystallinity section, which remains even through the biodegradation process (Rosli et al., 2021; Kalita et al., 2021). In composite materials, increased weight loss percentages correspond to increased fiber content. Natural fibers such as cellulose and hemicellulose have hydrophilic qualities, which means they have the potential to absorb water and degrade at a faster pace when used in composite materials (Zandi et al., 2019; Alias et al., 2021; Rosdi, Salim, Roslan, Bakar, and Sarmin, 2023). Because of increased water

absorption, the molecular chain of PLA in the composites experienced hydrolytic degradation and became shorter. Microorganisms can assimilate small molecules during the degradation process. As a result, the PLA/NR/RS biocomposite films exhibited higher rates of deterioration. The initial stage of degradation for all films seems to be rather slow, with a more significant decomposition starting in the next few months. The PLA/NR/RS bio-composite films still exhibited a greater rate of degradation. Therefore, using films, particularly PLA/NR/RS biocomposites at 5 wt.%, presents an interesting option for future use. Table 4.4 provides a summary of the weight loss percentage in neat PLA, PLA/NR blend, and PLA/NR/RS biocomposite films following a 90-day soil burial period.

Table 4.4 Summary of weight loss percentage of the neat PLA, PLA/NR blend, and PLA/NR/RS biocomposite films after being buried in soil for 90 days.

Sample	Weight loss (%)
Neat PLA	3.33 ± 0.32
PLA/NR blend	4.20 ± 1.02
PLA/NR/3%RS	4.54 ± 0.42
PLA/NR/5%RS	8.29 ± 0.43

4.3.2.2 Molecular weight determination using GPC technique

The neat PLA and the PLA phase in PLA/NR blend, and PLA/NR/RS biocomposite film samples were analyzed using GPC both before and after degradation investigations. The results obtained from the analysis are shown in Table 4.5. An observed reduction in the molecular weight of the PLA phase occurred after 90 days of soil burial biodegradation. This observation is consistent with earlier investigations (Juntuek, Chumsamrong, Ruksakulpiwat, and Ruksakulpiwat, 2015; Vasile et al., 2018). Moreover, the addition of NR and RS to the PLA matrix has led to a further decrease in the average molecular weight. This result corresponds to the results obtained from the analysis of weight loss percentages in PLA/NR blend and PLA/NR/RS bio-composite films. Similar results were obtained by Pongputthipat et al. (2023), who reported a decrease in the molecular weight of PLA when rice straw was added to the

PLA/NR blend. This addition of rice straw was found to increase PLA hydrolysis (Sakai et al., 2011).

Table 4.5 The number-average molecular weights (Mn), weight-average molecular weights (Mw), and polydispersity index (PDI) of neat PLA, PLA extracted from each film were determined before and after being buried in soil for 90 days.

Sample	Before burial in soil			After burial in soil		
	Mn (g/mol)	Mw (g/mol)	PDI	Mn (g/mol)	Mw (g/mol)	PDI
Neat PLA	38,487	160,328	4.17	35,983	153,098	4.25
PLA/NR	33,510	84,639	2.52	31,800	84,183	2.65
PLA/NR/3%RS	32,132	80,510	2.50	29,332	73,050	2.49
PLA/NR/5%RS	30,039	70,716	2.35	28,211	72,781	2.58

4.3.2.3 Tensile properties

Figure 4.11 (a-b) shows the tensile stress-strain curves of neat PLA, PLA/NR blend, and PLA/NR/RS biocomposites after being buried in soil for 90 days. The fracture behavior of both the neat PLA and PLA/NR blend in machine direction (MD) was like that before burial, with neat PLA displaying a brittle fracture and PLA/NR blend displaying a ductile fracture. PLA/NR/RS biocomposite exhibits a transition from ductile to brittle fractures. The transverse direction (TD) of both neat PLA and PLA/NR/RS biocomposite exhibit lower stress-strain curve compared to the machine direction (MD). However, both directions show a similar pattern. It is worth noting that the PLA/NR blend tends to be more brittle. The tensile strength of neat PLA, PLA/NR blend, and PLA/NR/RS biocomposite films before and after the soil burial test for 90 days are compared in Figure 4.12 (a-b). After being buried in the soil for a period of 90 days, it was seen that the tensile strength of neat PLA, PLA/NR blend, and PLA/NR/RS biocomposite films decreased. The observed outcome is a consequence of the deterioration of the films that takes place throughout the process of soil burial. During the process of decomposition in a landfill, the chain structure of films may undergo a breakdown and the formation of pores on the surface. This leads to concentrated

stress around these pores, which reduces their ability to support loads and finally results in a decrease in tensile strength (Chuayjuljit, Wongwaiwattanakul, Chaiwutthinan, and Prasassarakich, 2016; Zhang, Cao, and Jiang, 2023). The presence of NR and RS fiber will enhance the breakdown process. It is evident that the addition of NR and fibers resulted in more of a decrease in tensile strength compared to the case without them. However, a pattern that is similar can be seen in both MD and TD directions.

Figure 4.13 (a-b) shows the elongation at break of neat PLA, PLA/NR blend, and PLA/NR/RS biocomposites before and after soil burial testing. The elongation at break exhibited the same trend as the trend observed in tensile strength. It was observed that the elongation at break has exhibited significant changes in PLA/NR blend, and PLA/NR/RS biocomposite.

Young's moludus of neat PLA, PLA/NR blend, and PLA/NR/RS biocomposite films before and after soil burial testing are shown in Figure 4.14 (a-b). Which found that modulus of all films is increased especially PLA/NR/RS biocomposite films. It is seen that the modulus of all films has increased, especially in the case of PLA/NR/RS biocomposite films. The presence of RS fiber results in rapid deterioration due to the high probability of natural fibers being subjected to hydrolytic degradation by soil microbes such as fungus and bacteria (Brunsek, Kopitar, Schwarz, and Marasovic, 2023). The initial step of PLA degradation is well recognized to involve crystallization within its structure. Usually, natural fibers act as natural nucleating agents (Lubos, Martin, and Jozef, 2014), leading to enhanced crystallinity and a more compacted arrangement of polymer chains. Consequently, this results in an increase in modulus. Similar patterns have been observed in both the MD and TD directions.

Following 90 days of soil burial, the tensile strength, Young's modulus, and elongation at break of the neat PLA, PLA/NR blend, and PLA/NR/RS biocomposite films are summarized in Table 4.6.

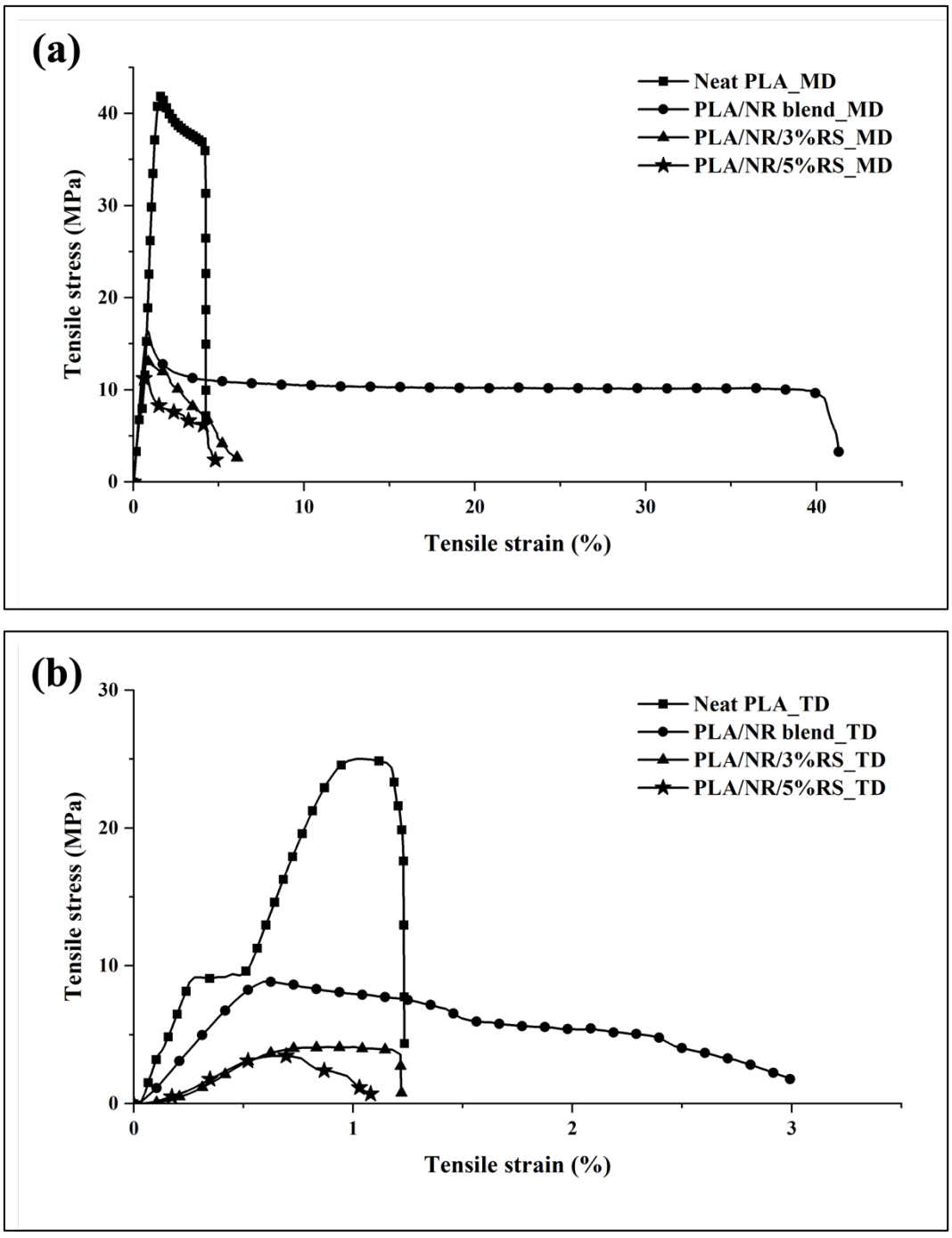

Figure 4.11 Stress-strain curve of neat PLA, PLA/NR, and PLA/NR/RS biocomposite films; machine direction (MD) (a) and transverse direction (TD) (b) after being buried in soil for 90 days.

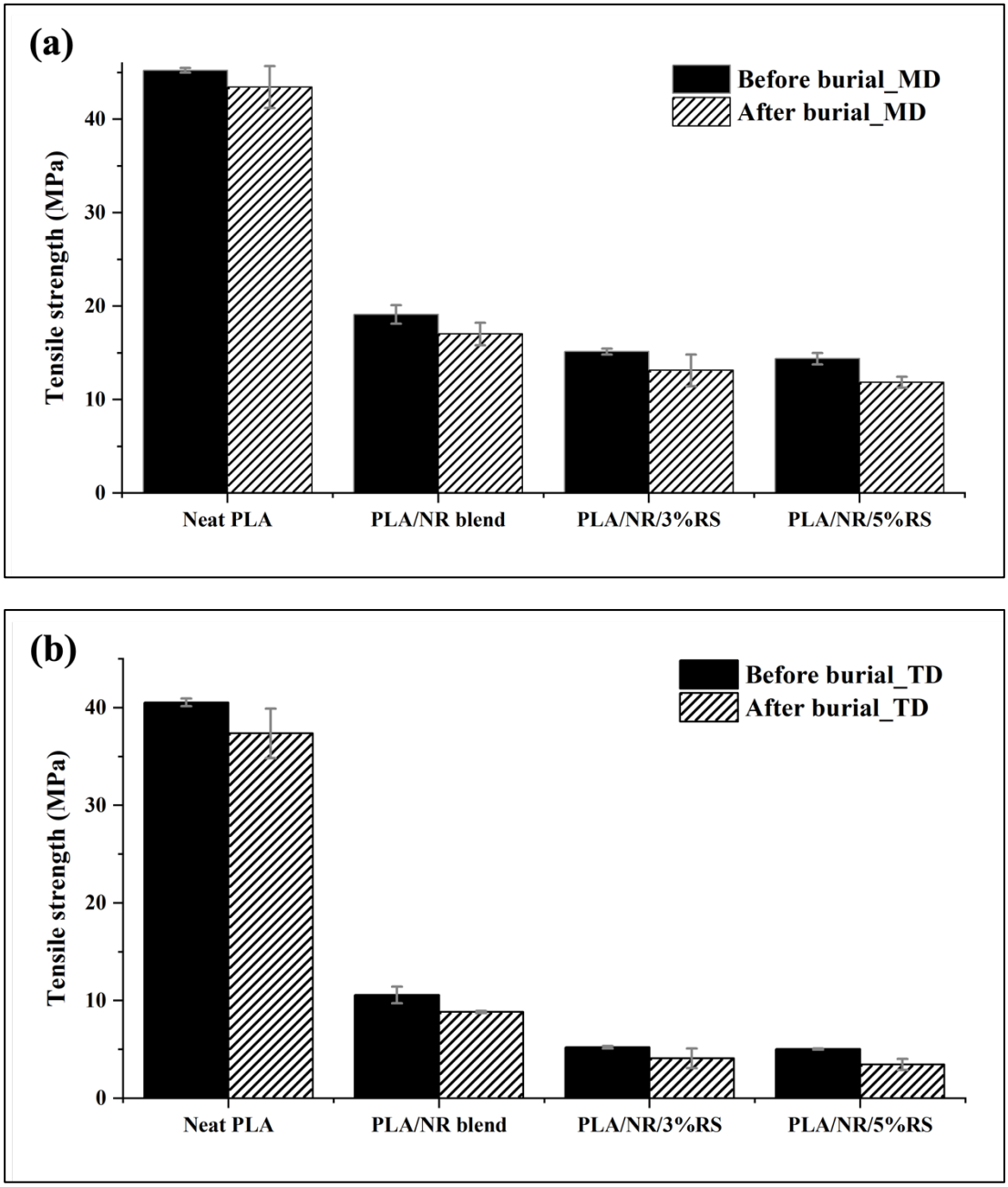

Figure 4.12 Tensile strength of neat PLA, PLA/NR blend, and PLA/NR/RS biocomposites films; MD (a), TD (b) before and after soil burial test for 90 days.

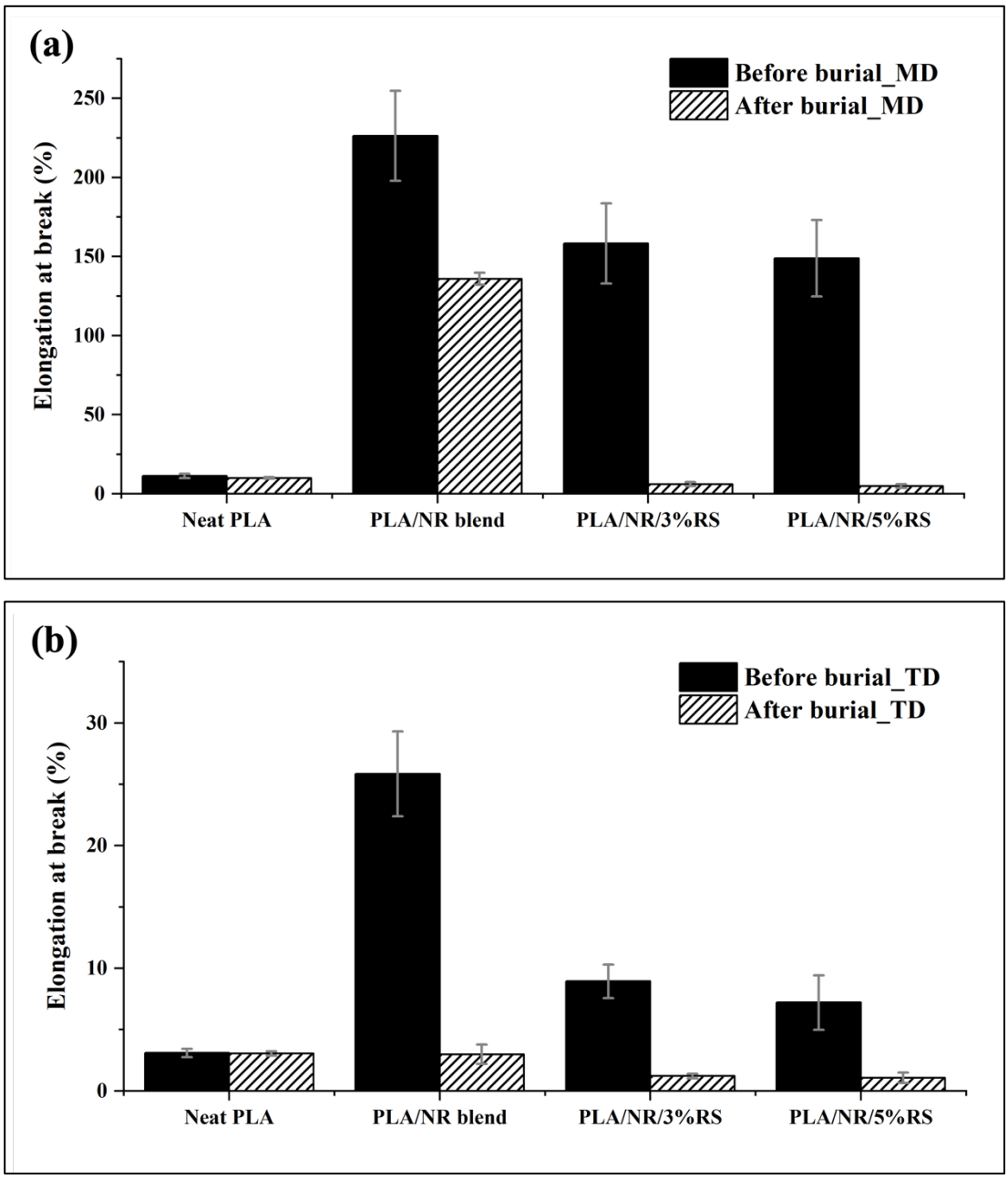

Figure 4.13 Elongation at break of neat PLA, PLA/NR blend, and PLA/NR/RS biocomposites films; MD (a), TD (b) before and after soil burial test for 90 days.

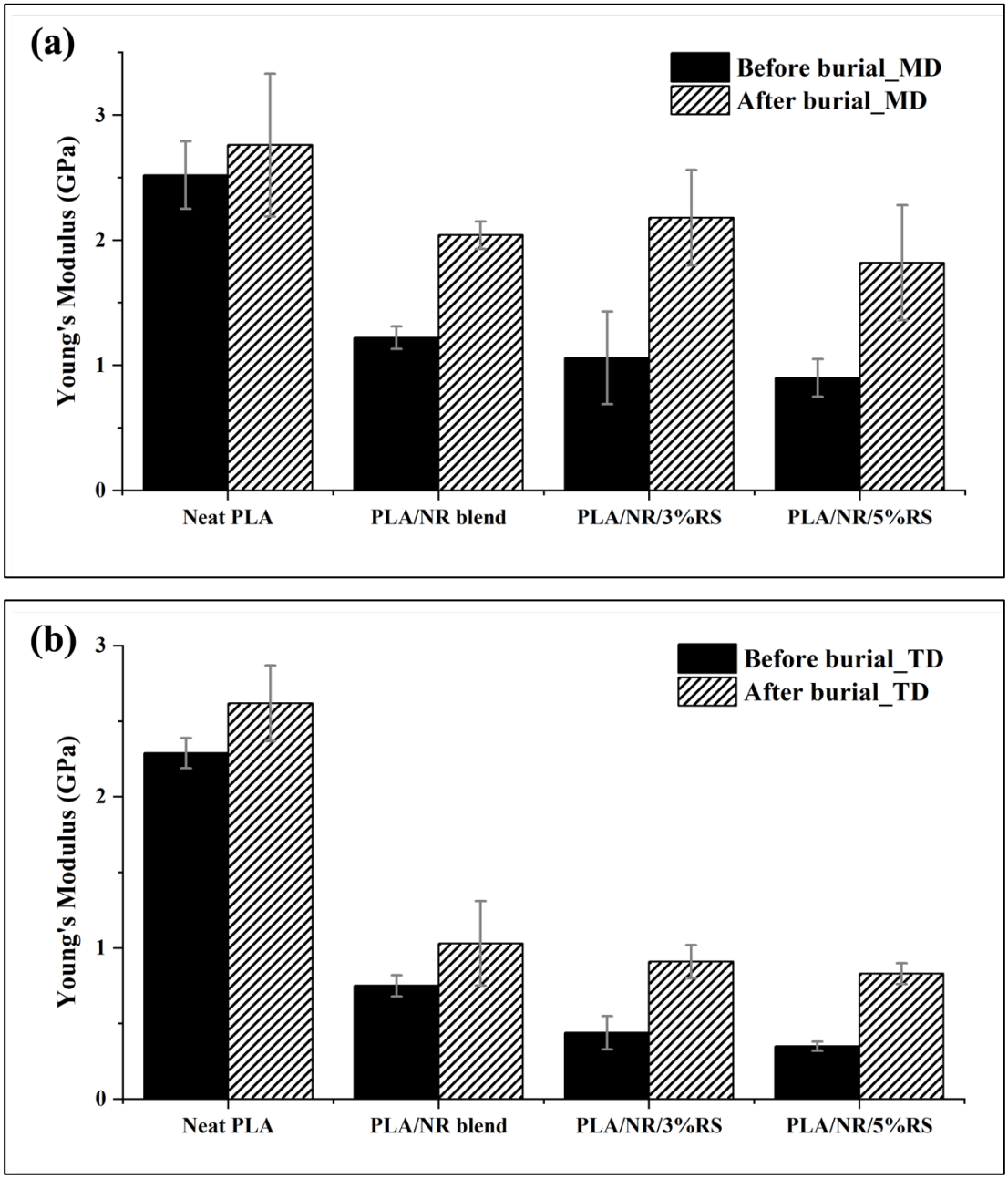

Figure 4.14 Young's Modulus of neat PLA, PLA/NR blend, and PLA/NR/RS biocomposites films; MD (a), TD (b) before and after soil burial test for 90 days.

Table 4.6 Summary of tensile properties of neat PLA, PLA/NR blend, and PLA/NR/RS biocomposite films after being buried in soil for 90 days.

Sample		Tensile Strength (MPa)	Young's Modulus (GPa)	Elongation at break (%)
Neat PLA	MD	41.87 ± 2.25	4.74 ± 0.57	4.25 ± 0.42
	TD	32.4 ± 2.54	3.61 ± 0.25	1.23 ± 0.17
PLA/NR blend	MD	16.42 ± 1.21	2.44 ± 0.11	41.30 ± 3.80
	TD	8.85 ± 0.11	1.62 ± 0.28	2.99 ± 0.79
PLA/NR/3%RS	MD	13.13 ± 1.70	2.18 ± 0.38	6.08 ± 1.30
	TD	4.09 ± 1.02	0.91 ± 0.11	1.22 ± 0.19
PLA/NR/5%RS	MD	11.85 ± 0.60	1.82 ± 0.46	4.80 ± 1.21
	TD	3.46 ± 0.58	0.83 ± 0.07	1.08 ± 0.43

4.3.2.4 Morphological properties

Figure 4.15 exhibits the FE-SEM micrographs of the surface characteristics of neat PLA, PLA/NR blend, and PLA/NR/RS biocomposite films before they were exposed to soil burial. The PLA film had a smooth surface, whereas the PLA/NR blend and PLA/NR/RS biocomposite had a rough surface and a heterogeneous phase surface. This phenomenon occurs because of PLA and NR polymers' immiscibility.

After a 90-day period of soil burial, the morphology of all films underwent alterations, as depicted in Figure 4.16. The surfaces of the neat PLA, PLA/NR blend, and PLA/NR/RS biocomposite films exhibited numerous fractures and pores, along with evident indications of fungal growth on the blend and composite film surfaces. The findings are consistent with previous research that observed the presence of bacterial and fungal propagules, including reproductive hyphae and spores, on deteriorating plastic surfaces (Sriyapai, Chansiri, and Sriyapai, 2018; Gkoutselis et al., 2021).

Furthermore, the incorporation of RS into PLA has been seen to lead to an augmentation in fungal populations, accompanied by an expansion in their size (Banthao, Kumpolsan, Baimark, Wongkasemjit, and Pakkethati, 2020). The

water absorption property of RS results in the swelling of the polymer, hence increasing microbial attack and intensifying microbial activity. The increase in microbial activity is dependent upon the existence of both water and oxygen (Yaacob, Ismail, and Ting, 2016).

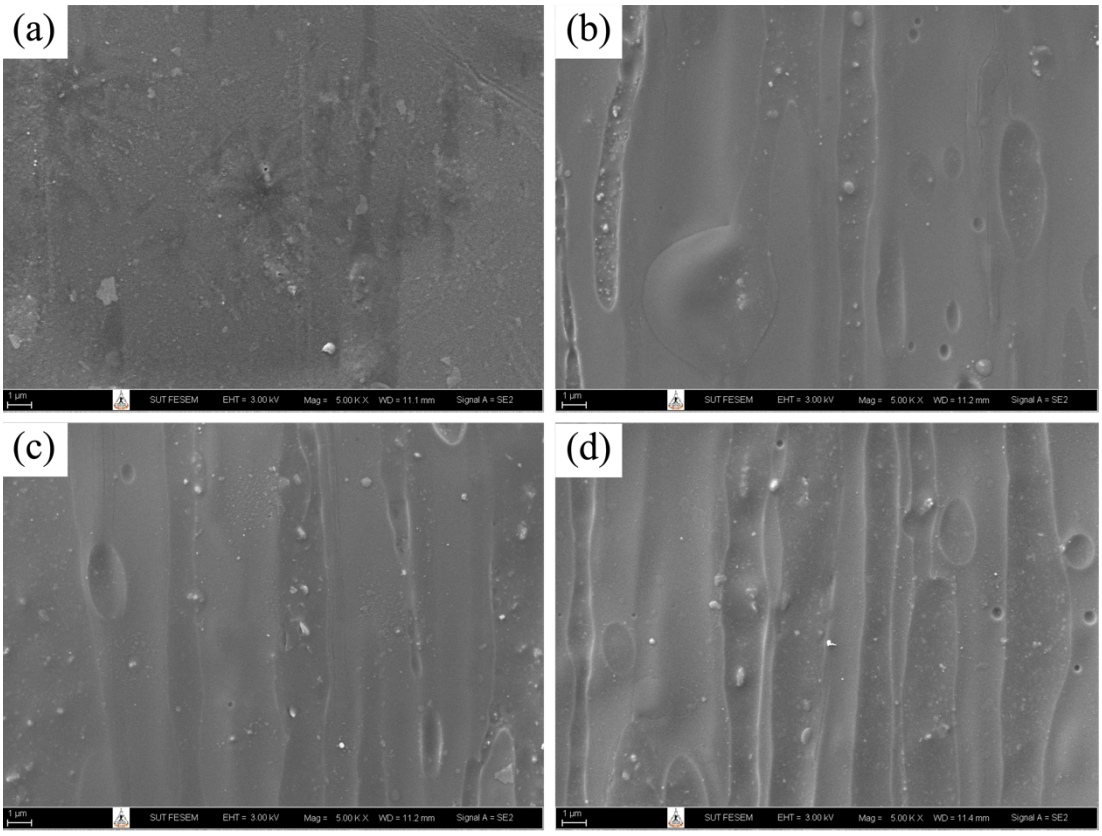

Figure 4.15 FE-SEM micrographs at 5000x magnification of film surface of neat PLA (a) PLA/NR blend (b), and PLA/NR/RS biocomposite films at RS contents of; 3 wt.% (c), and 5 wt.% (d).

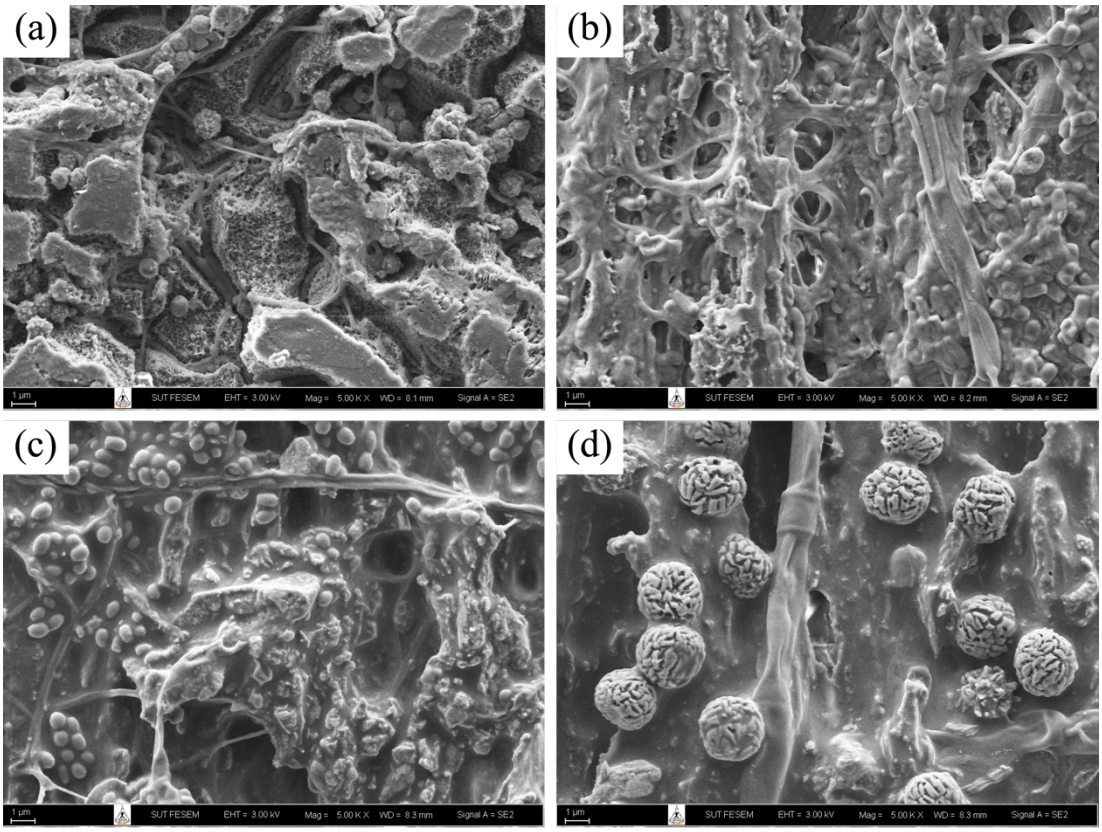

Figure 4.16 FE-SEM micrographs at 5000x magnification of film surface after soil burial for 90 days of neat PLA (a) PLA/NR blend (b), and PLA/NR/RS biocomposite films at RS contents of; 3 wt.% (c), and 5 wt.% (d).

4.3.2.5 EDX analysis

Table 4 displays the data revealing that the primary elements present in the neat PLA, PLA/NR blend, and PLA/NR/RS biocomposite samples, prior to being buried in soil, were carbon (C) and oxygen (O). Nitrogen (N) was detected after a 90-day interval of soil burial. The presence of nitrogen can be attributed to the emission of biological substances from fungal spores, particularly proteins (Diaz-Hernandez, Sanchez-Soto, and Serrano-Delgado, 2012). Nitrogen is an essential component of plant nucleic acids, enzymes, and proteins, and it provides an important role in assisting several metabolic pathways following degradation (Yadav and Kumar, 2023). Moreover, it was discovered that the C content dropped after the burial of all polymer films in soil; in contrast, the O content increased. The observed reduction in carbon content confirms biodegradation, while the rise in oxygen percentage counteracts the decrease in carbon atomic percentage. This is evident that oxidation

processes are occurring on all polymers during the biodegradation process. (Wufuer, Li, Wang, and Duo, 2022).

Table 4.7 EDX analysis of element contents of neat PLA, PLA/NR blend, and PLA/NR/RS biocomposite films before and after in soil for 90 days.

Sample	Before burial in soil		After burial in soil		
	C/wt.%	O/wt.%	C/wt.%	O/wt.%	N/wt.%
Neat PLA	84.97	15.03	61.65	24.63	13.72
PLA/NR	75.33	24.67	55.27	31.35	13.38
PLA/NR/3%RS	73.93	26.08	53.14	33.21	13.65
PLA/NR/5%RS	74.12	25.89	51.36	32.89	15.75

4.3.2.6 DSC analysis

Differential scanning calorimetry (DSC) has been used to assess the thermal properties of polymers. Some of these characteristics include phase transitions, crystallisation behaviours, and thermal heat capacity. DSC simplifies the identification and analysis of degradation that occurs during polymer processing by facilitating the examination of changes in thermal properties (Velghe, Buffel, Vandeginste, Thielemans, and Desplentere, 2023). This study just analysed data from the first heating scan (Figure 4.17) to examine the structural changes of materials during using. The results showed the PLA in its crystalline form in the molded samples (Feng, Hu, Yin, Zhao, and Jiang, 2013). To investigate the thermal changes resulting from degradation, the glass transition temperature (Tg), melting temperature (Tm), cold crystallisation temperature (Tcc), and degree of crystallisation (Xc) of neat PLA, PLA/NR blend, and PLA/NR/RS biocomposite film samples were measured both before and after being buried in soil. The measured values are presented in Table 4.8.

The neat PLA demonstrated a Tg of 62.67°C. Upon the addition of NR to PLA, two different Tg values were identified at -67.68°C and 63.83°C. These values related to the NR and PLA phases, respectively. The presence of two glass transition temperatures can be attributed to the incompatibility of PLA and NR blends (Xu et al., 2014). The presence of two different crystalline forms in a polymer is indicated by the occurrence of two distinct melting points. The elevated temperature

at which the melting point was seen indicates a more well-defined crystalline structure. The presence of two distinct melting peaks in the PLA phase can be attributed to the transformation of alpha'-form crystals into alpha-form crystals (Taib et al., 2023). The incorporation of NR and RS into the PLA did not lead to any substantial change in the Tg and Tm values. Adding NR results in a reduction in Tcc, causing a transition towards lower temperatures. Prior research has shown that elastomers improve the mobility of polymer chains and accelerate the crystallization process in PLA (Thongpin et al., 2013; Burkov et al., 2021). After the addition of RS to the PLA/NR blend, there was a slight increase in Tcc, although it remained lower than that of the neat PLA. RS demonstrated potential as a nucleating agent, hence improving the crystallization process (Tisserat, Joshee, Mahapatra, Selling, and Finkenstadt, 2013; Bomfim et al, 2023). Furthermore, the addition of NR to PLA leads to a significant enhancement in crystallinity (Xc), and this increase is even more pronounced when RS is added. This is related to NR and RS, which can function as nucleating agents to enhance the crystallization process of PLA (Suksut and Deeprasertkul, 2011; Ming et al., 2015).

Table 4.8 DSC Results of neat PLA, PLA/NR blend, and PLA/NR/RS biocomposite films before and after burial in soil for 90 days.

Sample code	$Tg_{(NR)}$ (°C)	$Tg_{(PLA)}$ (°C)	Tcc (°C)	Tm_1 (°C)	Tm_2 (°C)	Xc (%)
Neat PLA Before	-	62.67	100.65	148.41	153.58	3.97
Neat PLA After	-	63.47	100.68	150.83	156.17	4.31
PLA/NR blend Before	-67.68	63.83	89.54	147.25	154.75	7.92
PLA/NR blend After	-67.78	63.16	91.18	147.42	155.25	9.62
PLA/NR/3%RS Before	-68.80	63.20	92.95	139.90	155.33	9.54
PLA/NR/3%RS After	-67.51	63.62	93.68	144.20	155.92	10.78
PLA/NR/5%RS Before	-68.24	62.53	91.60	145.01	155.08	11.63
PLA/NR/5%RS After	-67.69	63.37	93.63	147.67	158.92	13.03

After a 90-day duration of soil burial, the Tg of all polymers remained unchanged, indicating that the soil burial had no effect on the Tg of the polymers. The degradation process resulted in an increase of 1-3 °C in both Tcc and Tm. All polymers showed an increase in crystallinity (Xc), with blends and composites exhibiting a somewhat higher level. NR and RS can enhance the degradation process by increasing the absorption of water into the less resistant amorphous phase, which is often more susceptible to microbial activity and hydrolysis compared to the crystalline phases. This action disrupted molecule bonds in the amorphous regions, enabling the motion and rearrangement of the remaining molecular bonds into a crystalline structure (Yaacob et al., 2016; Lv, Zhang, Gu, and Tan, 2018; Silva, Pereira, Passador, and Montagna, 2020).

4.3.2.7 XRD analysis

X-ray diffraction (XRD) analysis was employed to monitor transformations in the crystalline structure of the polymers attributed to degradation. Figure 4.18 displays the XRD patterns of the samples before and after a 90-day burial in soil. The XRD patterns of PLA showed a broad peak at about $2\theta = 16°$, indicating there were no clear diffraction peaks and confirming that its structure was mostly amorphous (Palsikowski, Kuchnier, Pinheiro, and Morales, 2017). The results obtained correspond to the DSC analysis's findings, which revealed a significantly low degree of crystallinity. The XRD examination identified the low degree of crystallinity. The PLA/NR blend and the PLA/NR/RS biocomposite both had clear diffraction peaks at $2\theta = 10°$ and $2\theta = 28°$ on the XRD pattern. These findings suggest that the presence of NR and RS influences the crystalline structure of PLA. The intensity of all diffraction peaks increased after being buried in the soil, as did the increase in RS content. As the RS content increased, the composites exhibited more degradation, resulting in the generation of more low-molecular-weight chains. As a result, molecular mobility increased, and diffraction peaks became more intense. This phenomenon has also been reported in PLA/starch composites (Lv et al., 2017). The finding accords with the previously indicated decrease in weight loss percentage and molecular weight.

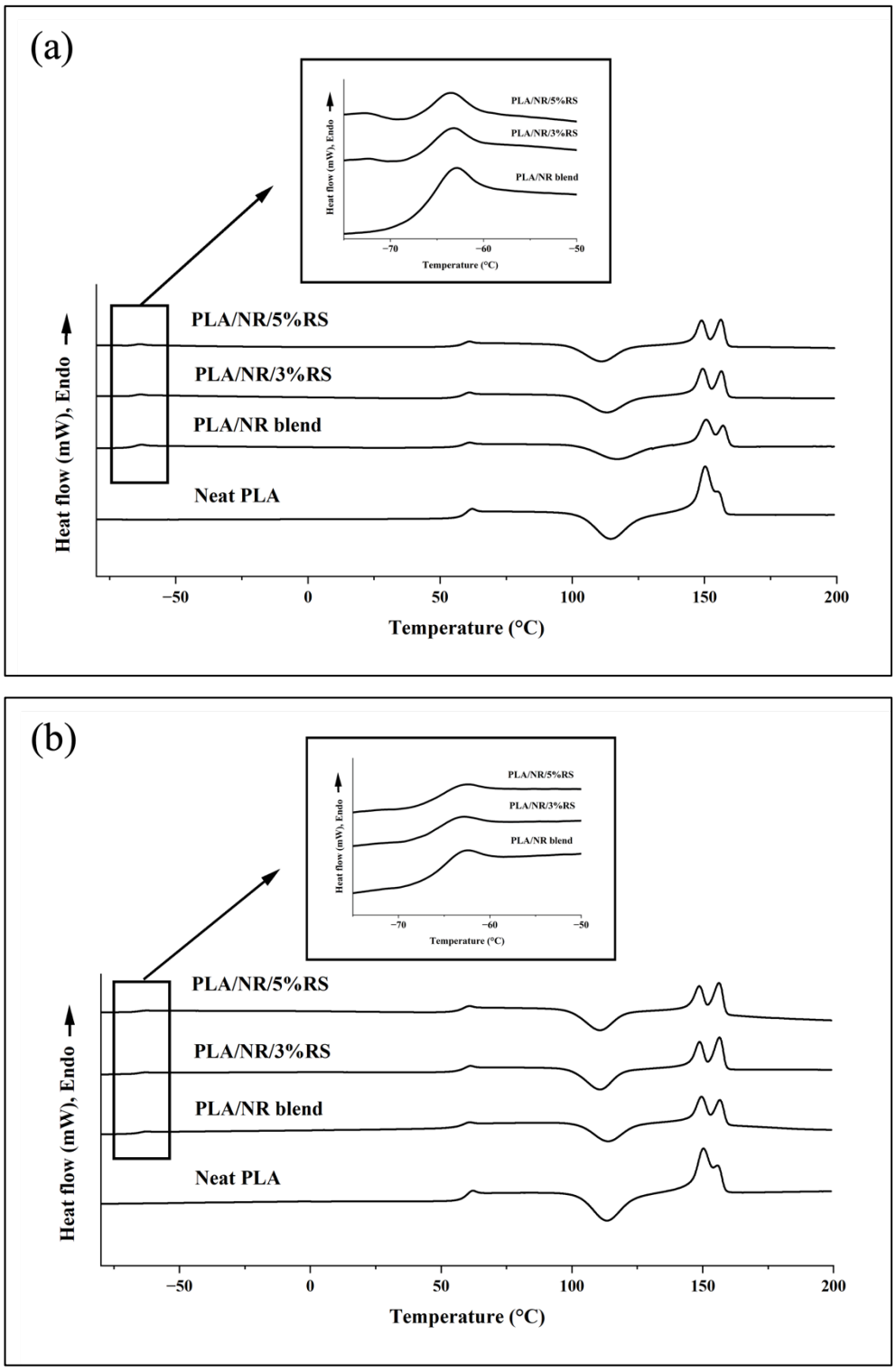

Figure 4.17 DSC thermograms of neat PLA, PLA/NR blend, PLA/NR/3%RS, and PLA/NR/5%RS biocomposite films before (a) and after (b) burial in soil for 90 days.

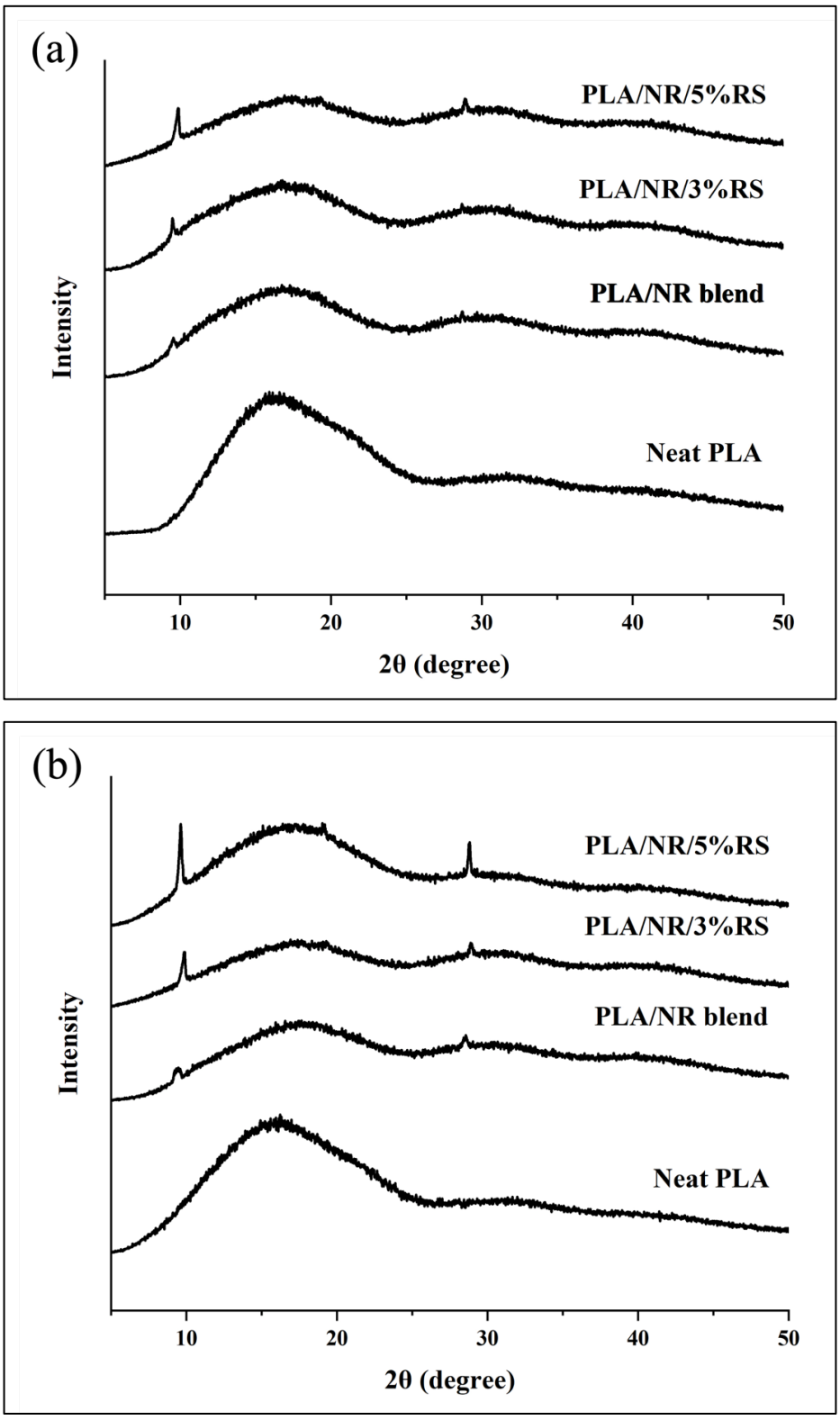

Figure 4.18 XRD patterns of neat PLA, PLA/NR blend, PLA/NR/3%RS, and PLA/NR/5%RS biocomposite films before (a) and after (b) burial in soil for 90 days.

4.4 Examples of Agricultural Applications of the biocomposite films

4.4.1 Seedling bags

The neat PLA, PLA/NR blend, and PLA/NR/RS biocomposite films were utilized to produce a seedling bag measuring 10x15 cm, with holes of approximately 0.5 cm in diameter, as shown in Figure 4.19. Chili plants were cultivated in seedling bags, which were then placed in a plant pot filled with soil for a period of 3 months, starting on August 7th, and finishing on November 7th, 2023. Figure 4.20 shows the first day of the chili planting. The progress of the chili's growth can be visually seen in Figures 4.21, 4.22, and 4.23, which correspond to time periods of 1, 2, and 3 months, respectively. The results from observing the growth of the chili plant's root in seedling bags after 90 days of planting are depicted in Figure 4.24.

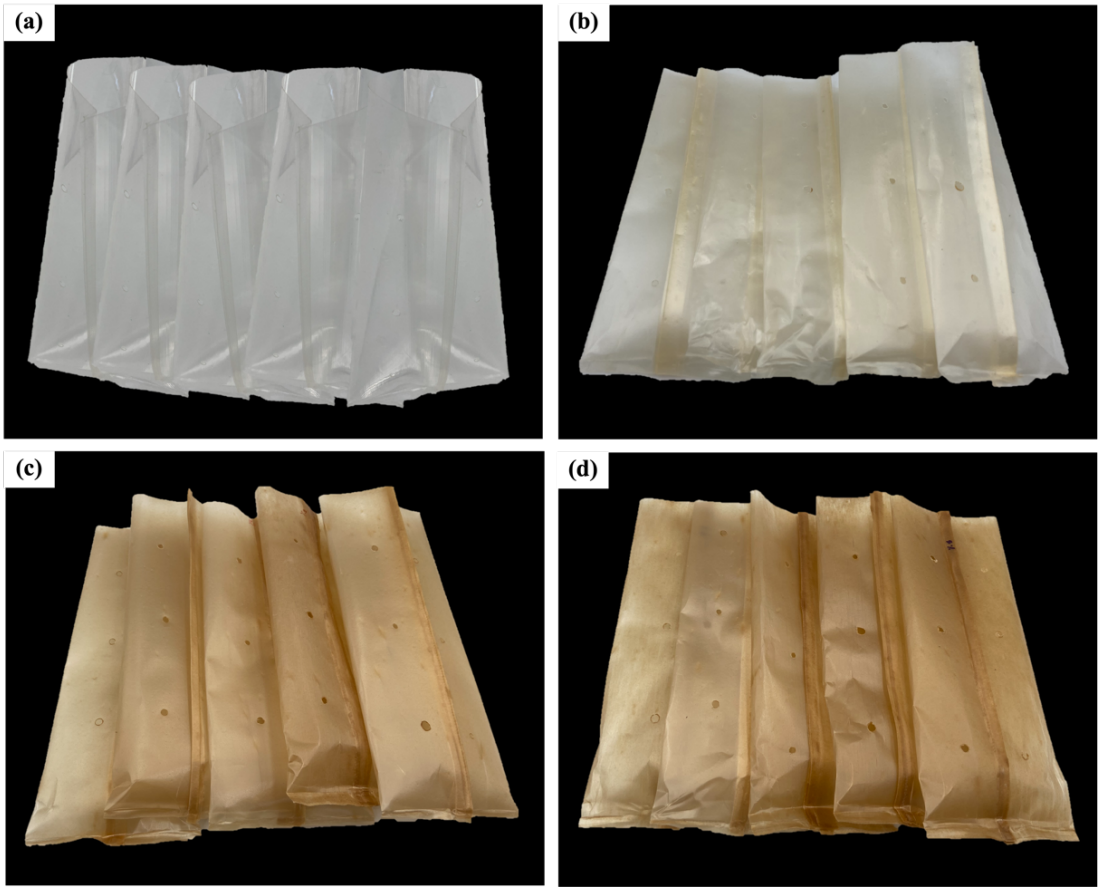

Figure 4.19 Seedling bags produced from neat PLA (a), PLA/NR blend (b), PLA/NR/3%RS (d), and PLA/NR/5%RS (e) biocomposite films.

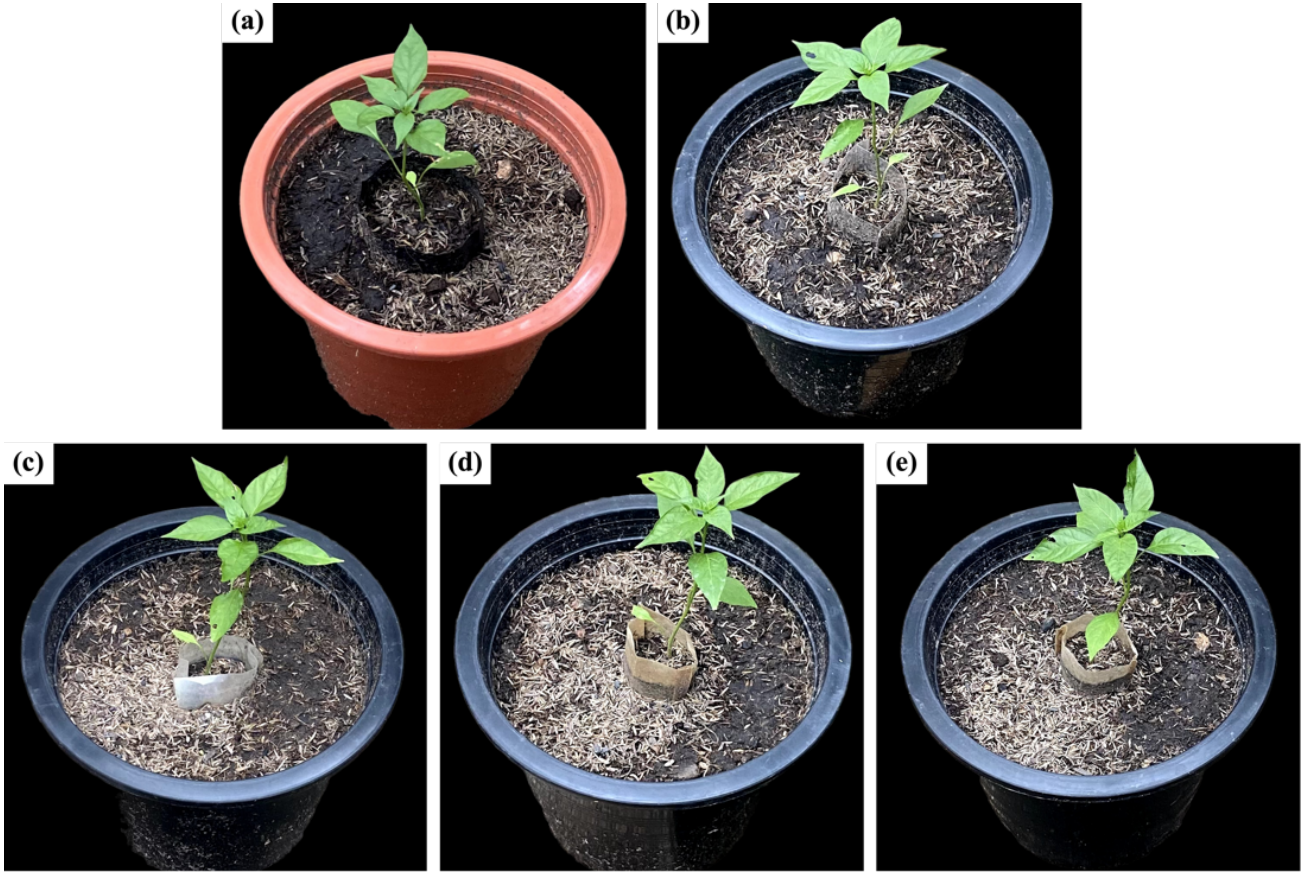

Figure 4.20 Chilli plants in seedling bags made from different types of film: (a) HDPE, (b) neat PLA, (c) PLA/NR blend, (d) PLA/NR/3%RS, and (e) PLA/NR/5%RS at 0 month. (All bags were placed in a plant pot filled with soil.)

Figure 4.21 Chilli plants in seedling bag made from HDPE (a), neat PLA (b), PLA/NR blend (c), PLA/NR/3%RS (d), and PLA/NR/5%RS (e) biocomposite films at 1 month of cultivation.

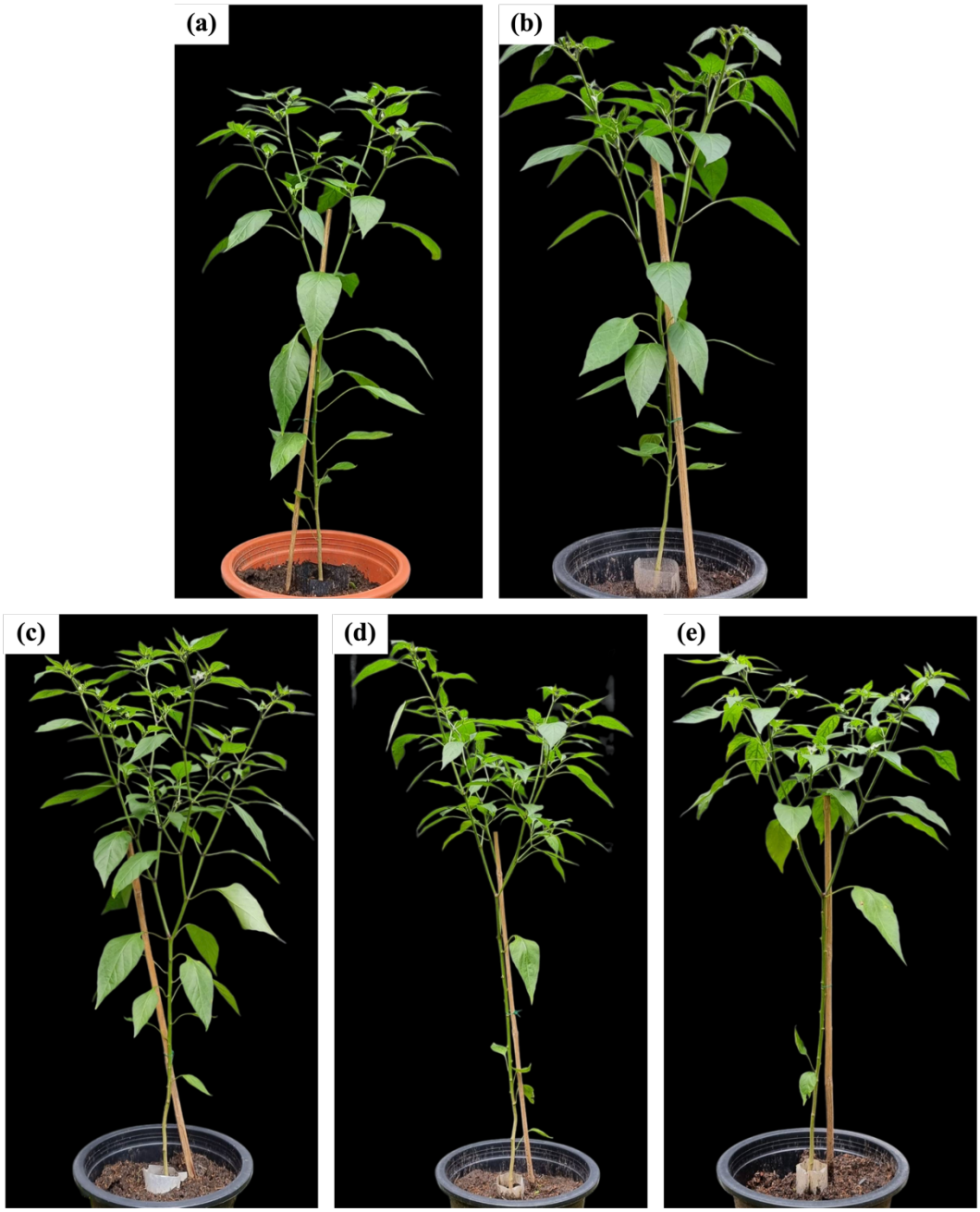

Figure 4.22 Chilli plants in seedling bag made from HDPE (a), neat PLA (b), PLA/NR blend (c), PLA/NR/3%RS (d), and PLA/NR/5%RS (e) biocomposite films at 2 months of cultivation.

Figure 4.23 Chilli plants in seedling bag made from HDPE (a), neat PLA (b), PLA/NR blend (c), PLA/NR/3%RS (d), and PLA/NR/5%RS (e) biocomposite films at 3 months of cultivation.

After a period of 3 months, it was discovered that the roots had grown out (as shown in Figure 4.24) and caused significant damage to the seedling bags, especially those made of PLA/NR blend and PLA/NR/RS biocomposite films. These bags exhibited significant tearing in comparison with the bags made of HDPE and neat PLA. The root penetration provides an indicator of the efficacy of the seedling bags, which can facilitate plant growth. During the planting process, the seedling bags can be put directly into the ground without being required to pull it off. This will have

no impact on the plant's root system. The bags can biodegrade organically, naturally breaking down within a suitable timeframe for each plant species.

To examine the influence of seedling bags on the growth of chili plants, multiple parameters, including dry weight, total weight of chili fruits, stem diameter, and height, were evaluated following a 3-month period of growth in the bags. Furthermore, the biodegradation of the seedling bags was investigated once the growth of the chili plant was completed.

Figure 4.24 The growth of chili plant’s root from seedling bags made from HDPE (a), neat PLA (b), PLA/NR blend (c), PLA/NR/3%RS (d), and PLA/NR/5%RS (e) biocomposite films after planting for 3 months.

4.4.1.1 Dry weight, total weight of chili fruits per plant, stem diameter and height of chili plants

The use of seedling bags made from neat PLA, PLA/NR blend, and PLA/NR/RS biocomposite films in a 3-month chili planting experiment did not affect the growth of the plants, compared to traditional seedling bags made from HDPE. The chili plants grown in bags made from a blend of PLA/NR and biocomposite films of PLA/NR/RS had a higher dry weight, total weight of chili fruit per plant (Figure 4.25), stem size, and height (Figure 4.26) than plants grown in HDPE and neat PLA bags. As a result, the plants exhibited faster development. This could be due to the roots' ability to penetrate the bag and spread into the surrounding soil. Typically, when a plant's root system grows completely and becomes strong, it will lead to the development of a healthy stem and leaf system.

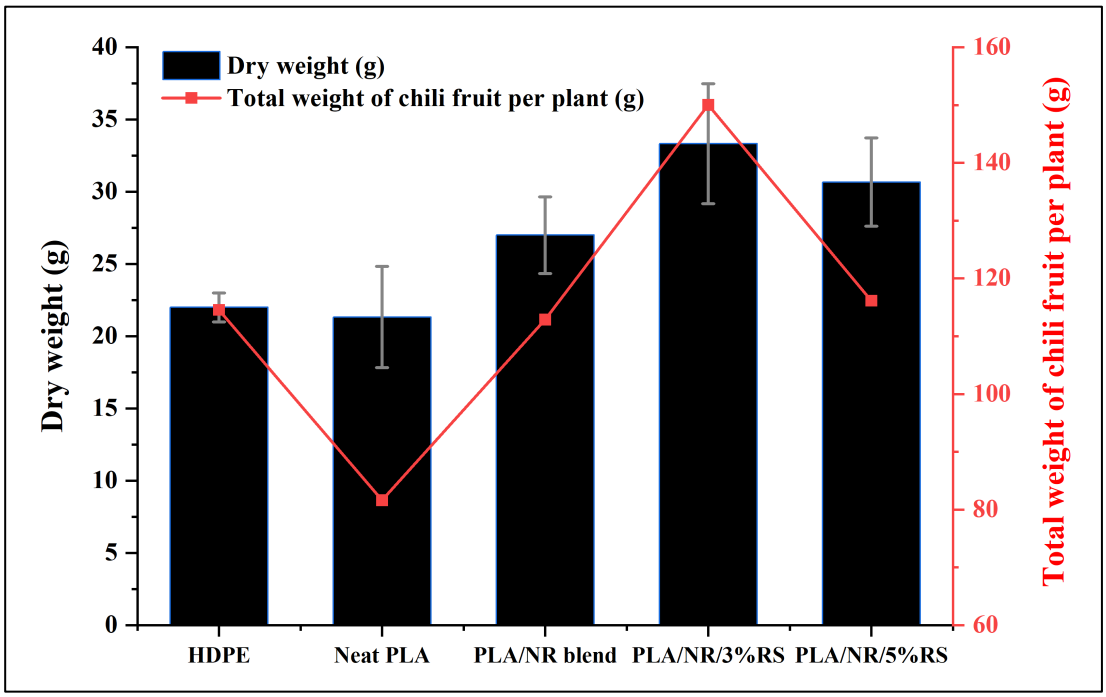

Figure 4.25 Comparison of the average dry weight and total weight of chili fruit per plant of the chili plant grown in different types of seedling bags for a period of 3 months.

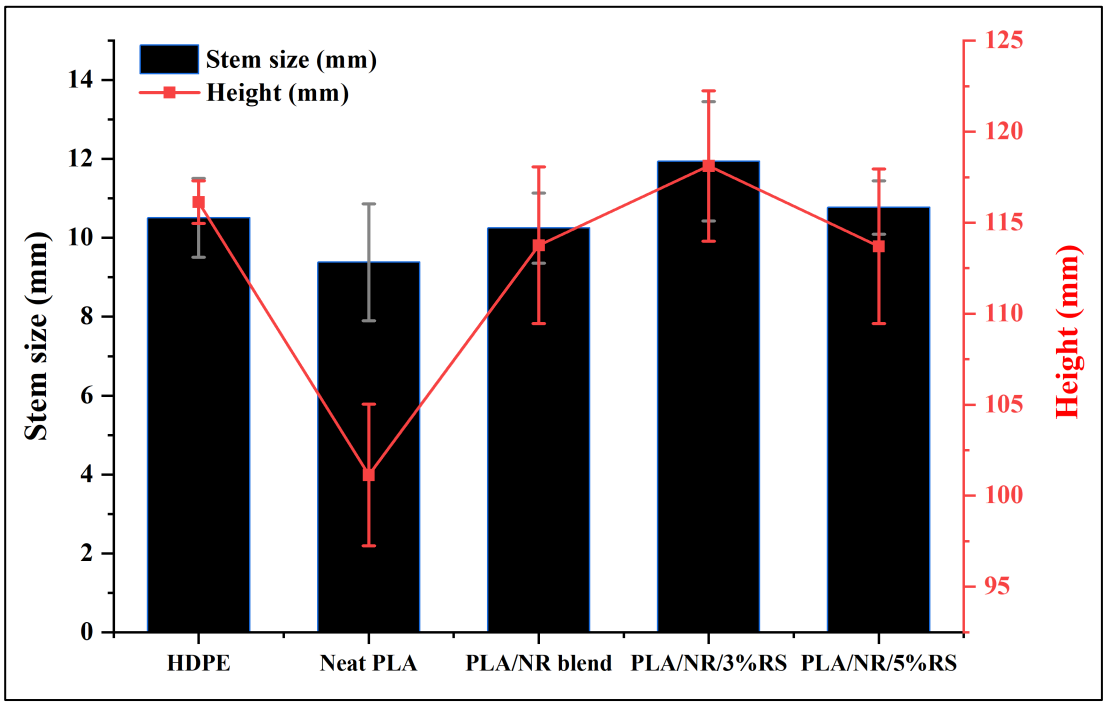

Figure 4.26 Comparison of the stem size and height of the chili plant grown in different types of seedling bags for a period of 3 months.

4.4.1.2 Biodegradation of seedling bags

4.4.1.2.1 Weight loss percentage

Figure 4.27 shows the percentage weight loss of the film samples after they had been shaped into seedling bags. The seedling bags made from PLA/NR/RS biocomposite film with 5% RS exhibited the highest percentage change in weight, determining 11.29 ± 0.37%. This was followed by PLA/NR/3%RS and PLA/NR blend, which showed weight losses of 8.48 ± 0.14% and 4.36 ± 0.24%, respectively. In contrast, neat PLA demonstrated low weight changes of 0.52 ± 0.08%. The weight loss percentage of seedling bags showed the same trend as the results of test films buried in the soil (Figure 4.10, page 58), with the seedling bag results being higher than the burial test.

PLA degradation primarily occurs through hydrolytic and microorganism activities, which are accelerated by humidity and water absorption. During the planting seed test using seedling bags, the film will be watered daily. Furthermore, the presence of NR and fibers improves the efficiency of the water absorption process. Because of increased water absorption, the PLA polymer chains in

the composite break down into smaller molecules. Another thing is that the presence of microorganisms is influenced by humidity, and microbes can assimilate small molecules during the process of decomposition. As a result, it enhances the degradation of the seedling bags in comparison to films buried in the soil with only 30% moisture content. Moreover, the act of roots penetrating the seedling bags causes damage. As a result, deteriorating films may have a larger surface area available for water absorption.

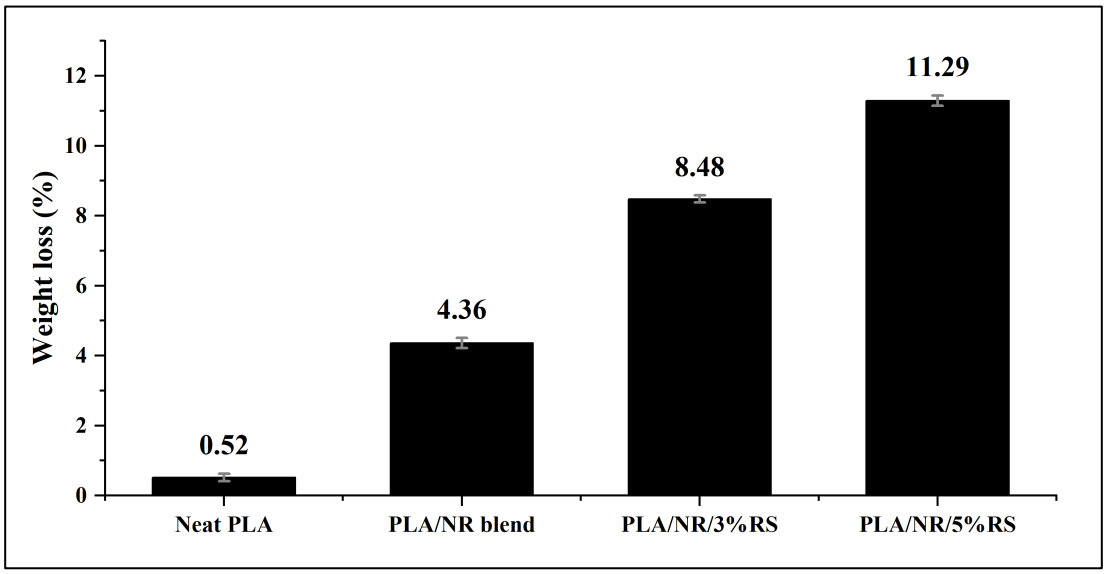

Figure 4.27 Weight loss percentage of seedling bags produced from neat PLA, PLA/NR blend, and PLA/NR/RS biocomposite films after planting for 3 months.

4.4.1.2.2 Molecular weight determination using GPC technique

After cultivating chili plants for three months, the PLA phase was extracted from all bags and subjected to analysis using the GPC technique. This analysis aimed to evaluate the number-average molecular weights (Mn), weight-average molecular weights (Mw), and polydispersity index (PDI). The analysis results listed in Table 4.9 indicate a significant reduction in the molecular weight of all films due to degradation.

Table 4.9 The number-average molecular weights (Mn), the weight-average molecular weights (Mw), and the polydispersity index (PDI) of neat PLA and the PLA extracted from PLA/NR blend and PLA/NR/RS biocomposite film, as well as from the films cut from seedling bags and mulch films after 3 months of chili plant growth.

Sample	Film (As prepared)			Seedling bag (After growing chili plants)			Mulch film (After growing chili plants)		
	Mn (g/mol)	Mw (g/mol)	PDI	Mn (g/mol)	Mw (g/mol)	PDI	Mn (g/mol)	Mw (g/mol)	PDI
Neat PLA	38,487	160,328	4.17	35,693	153,924	4.31	35,092	129,125	3.68
PLA/NR blend	33,510	84,639	2.52	31,114	85,135	2.74	28,413	67,654	2.38
PLA/NR/3%RS	32,132	80,510	2.50	29,501	82,802	2.81	28,398	72,651	2.56
PLA/NR/5%RS	30,039	70,716	2.35	28,906	72,209	2.50	27,916	67,169	2.41

The decrease in molecular weight corresponded to the decrease in weight loss, with a more significant decrease observed when NR and RS were added. Furthermore, it aligns with the results obtained from the investigation of the soil burial film test.

4.4.1.2.3 Tensile testing

The tensile properties of the film specimens cut from seedling bags produced from neat PLA, PLA/NR blend, and PLA/NR/RS biocomposite films were investigated before and after chili planting for 3 months to assess their degradability. The results are presented in Figure 4.28, and Table 4.10 shows the summary of the results. The tensile properties of any polymer undergo changes because of deterioration. The rate of degradation is influenced by various factors, including temperature, humidity, and the presence of microbes. The results showed that after using the film as a seedling bag for three months, both the tensile strength and the elongation at break decreased. This contrasts with the observed increase in Young's modulus. These results correspond to the results of the soil test for burial films, as shown in Table 4.6 (page 66). It can be observed that the test results acquired from seedling bags indicate that the film exhibits slightly more changes in mechanical properties compared to the film that was buried in the soil. These results are a direct consequence of the increased degradation caused by hydrolysis and microorganisms in the soil of the films. The film's surface deteriorates when the polymer structure chains are destroyed, leading to a loss in both tensile strength and elongation at break. An increase in Young's modulus is associated with an enhancement in the degree of crystallinity in the structure. The increase in crystallinity is a consequence of the degradation mechanism of PLA, so a rise in this property may suggest a higher rate of polymer degradation.

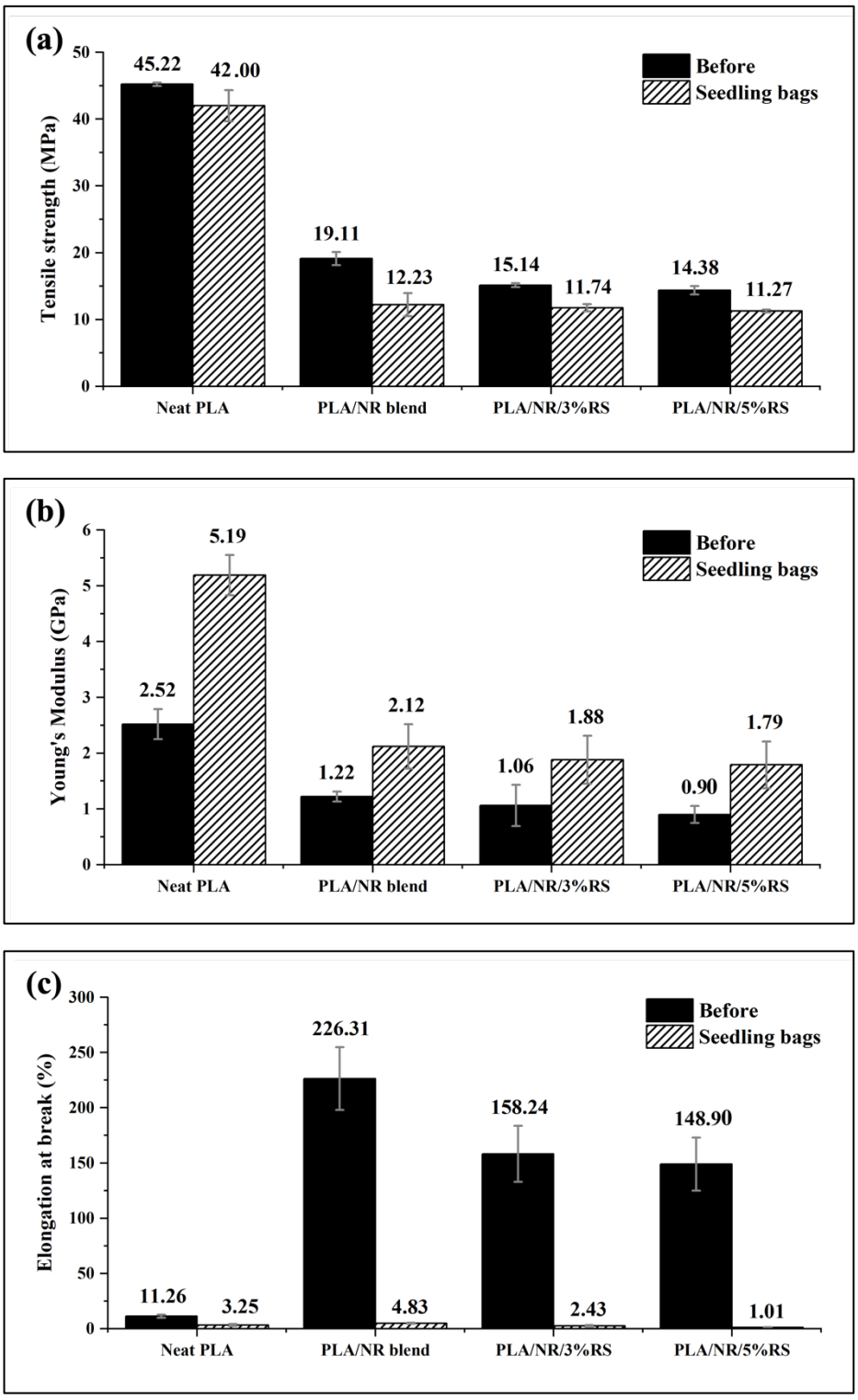

Figure 4.28 Tensile properties of the film specimens cut from seedling bags produced from HDPE, neat PLA, PLA/NR blend, and PLA/NR/RS biocomposites films; Tensile strength (a), Young's Modulus (b), and Elongation at break (c) before and after chili planting for 3 months.

Table 4.10 Summary of tensile properties of the film specimens cut from seedling bags produced from neat PLA, PLA/NR blend, and PLA/NR/RS biocomposite films after planting for 3 months.

Sample	Tensile Strength (MPa)	Young's Modulus (GPa)	Elongation at break (%)
Neat PLA	42.01 ± 2.32	5.19 ± 0.36	3.25 ± 0.85
PLA/NR blend	12.23 ± 1.72	2.12 ± 0.40	4.84 ± 0.44
PLA/NR/3%RS	11.75 ± 0.54	1.88 ± 043	2.43 ± 0.73
PLA/NR/5%RS	11.27 ± 0.21	1.79 ± 0.42	1.01 ± 0.32

4.4.1.2.1 Morphological properties

The FE-SEM micrographs show the surface characteristics of neat PLA, PLA/NR blend, and PLA/NR/RS biocomposite films after being used for seedling bags for a period of 3 months, as shown Figure 4.29. The figure shows that the surfaces of all films exhibit roughness and disorganized, indicating significant degradation of the surface. After the addition of NR and RS, it was discovered that the surface exhibited an increased presence of cracks and lacked smoothness. This confirms the increased degradation when NR and RS are added. The alteration in the surface characteristics of the film used for seedling bags was consistent with the film that had been buried in the soil for a duration of 3 months.

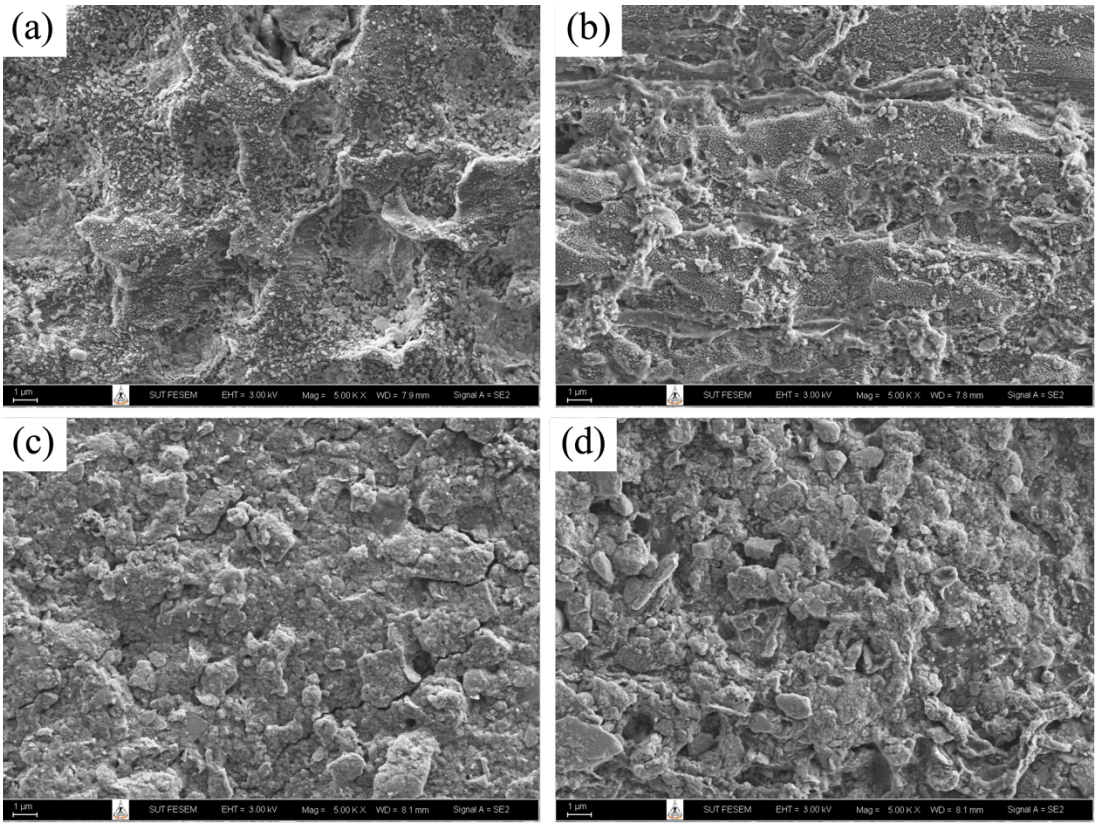

Figure 4.29 FE-SEM micrographs at 5000x magnification of the film specimens cut from seedling bags produced from neat PLA (a), PLA/NR blend (b), PLA/NR/3%RS (c) and PLA/NR/5%RS (d) biocomposite films after chili planting for 3 months.

4.4.1.2.2 DSC analysis

Figure 4.30 displays the DSC thermograms obtained during the first heating scan of the film samples taken from seedling bags, which were used for chili planting for a period of 3 months. This study investigated alterations in thermal characteristics during polymer degradation. An analysis revealed that the peak size of Tg increased in comparison to the DSC thermograms of the film sample before it was buried in soil for 3 months (Figure 4.17, page 72). This increase indicates the occurrence of a relaxation peak during the aging process, which arises when the sample is maintained at temperatures below its Tg for a long period of time (Parker, 2000). However, the transformation in Tg in almost all films did not demonstrate a significant shift when comparing films before and after their use as seeding bags for a period of 3

months, as shown in Table 4.11. Two distinct crystal forms were seen in the films that were used to produce the seedling bags, as indicated by the presence of two different Tm values. This crystal form represents a transformation in the crystal structure. From investigation, it was found that the alpha'- crystal form exhibited a reduced peak size, while the alpha- form crystals were larger in comparison to the before-buried film (Figure 4.17 (a), page 72). This result indicates a more organized and structured crystalline structure. Furthermore, the arrangement of the chain influences the decrease of the Tcc in all films. It was discovered that the value decreased in comparison to the value of the film that was not buried in the soil. The polymer's crystalline structure became more well-organized, resulting in a lower energy requirement for rearrangement. This leads to enhanced mobility of the polymer chains. Consequently, the polymer chains can be organized at lower temperatures (Maricilla and Beltran, 2017). Upon analyzing the crystallinity (Xc) of the PLA phase in the film samples taken from seedling bags used for growing chili plants for a duration of 3 months, it was observed that the Xc of the seedling bag films had increased. This finding aligns with the previously observed trend of increased Xc when the film is buried in soil.

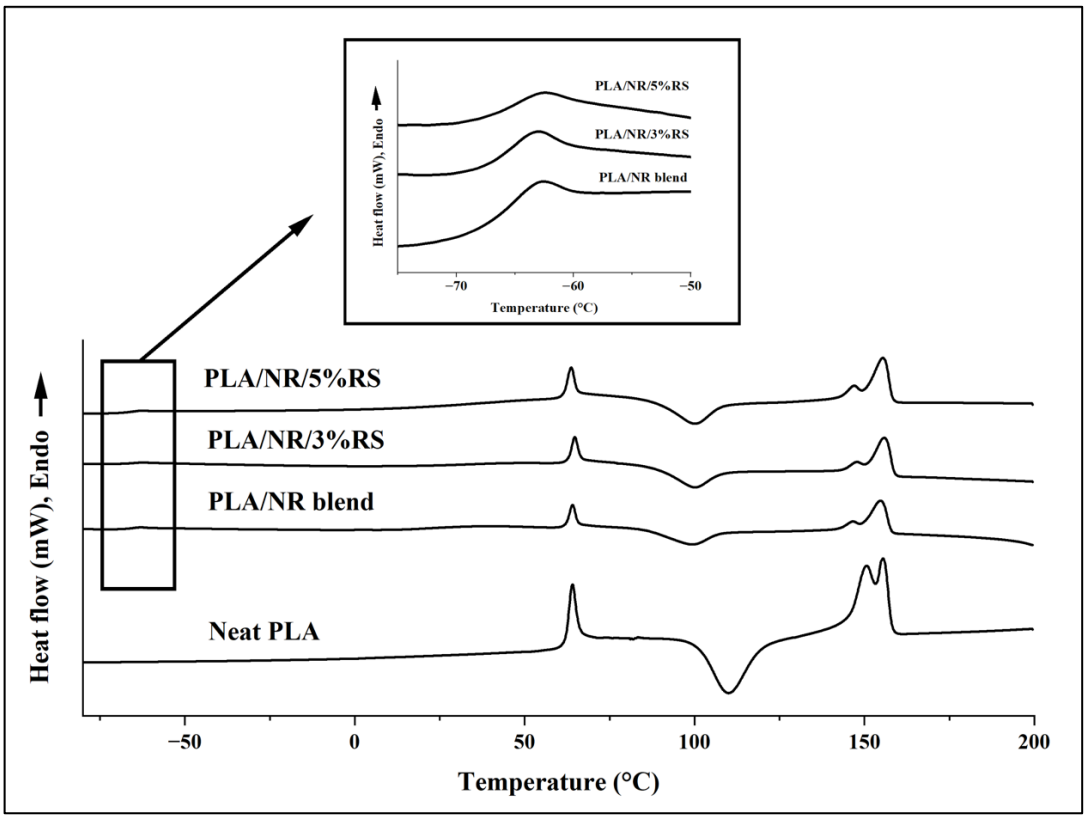

Figure 4.30 DSC thermograms of the samples taken from seedling bags after growing chili plants for a period of 3 months.

Table 4.11 The DSC results from the first heating scan of the cast film and the samples taken from seedling bags and mulch films after growing chili plants for 3 months.

Sample	Tg(NR) (°C)	Tg(PLA) (°C)	Tcc (°C)	Tm1 (°C)	Tm2 (°C)	Xc (%)
Neat PLA As prepared	-	62.67	100.65	148.41	153.58	3.97
Neat PLA Seedling bags	-	61.96	100.23	147.20	158.14	5.25
Neat PLA Mulch films	-	62.87	96.13	147.25	156.42	3.01
PLA/NR blend As prepared	-67.68	63.83	89.54	147.25	154.75	7.92
PLA/NR blend Seedling bags	-68.16	62.11	85.40	146.58	154.76	9.93
PLA/NR blend Mulch films	-66.27	60.10	86.27	-	154.75	7.68
PLA/NR/3%RS As prepared	-68.80	63.20	92.95	139.90	155.33	9.54
PLA/NR/3%RS Seedling bags	-67.96	62.78	88.71	144.94	155.83	10.49
PLA/NR/3%RS Mulch films	-	64.38	86.66	-	153.92	8.76
PLA/NR/5%RS As prepared	-68.24	62.53	91.60	145.01	155.08	11.63
PLA/NR/5%RS Seedling bags	-67.64	61.46	88.98	144.41	155.75	13.07
PLA/NR/5%RS Mulch films	-	63.70	83.64	-	152.92	10.02

4.4.1.2.3 XRD analysis

The XRD patterns, shown in Figure 4.31, indicated a change in the crystallinity of film samples taken from the seedling bags after a period of 3 months following chili planting. The neat PLA has a broad peak at 2θ degrees = 10°- 25°, which is attributed to the semicrystalline structure of PLA. The diffraction peaks of PLA/NR blend and PLA/NR/RS biocomposite films seen at 2θ degrees = 10° and 28°, corresponding with the test of film after being buried in soil (Figure 4.18 (b), page 73), indicate that PLA has undergone significant crystallization. It is possible that this is due to the presence of NR and RS, both nucleating agents that contribute to the degradation process.

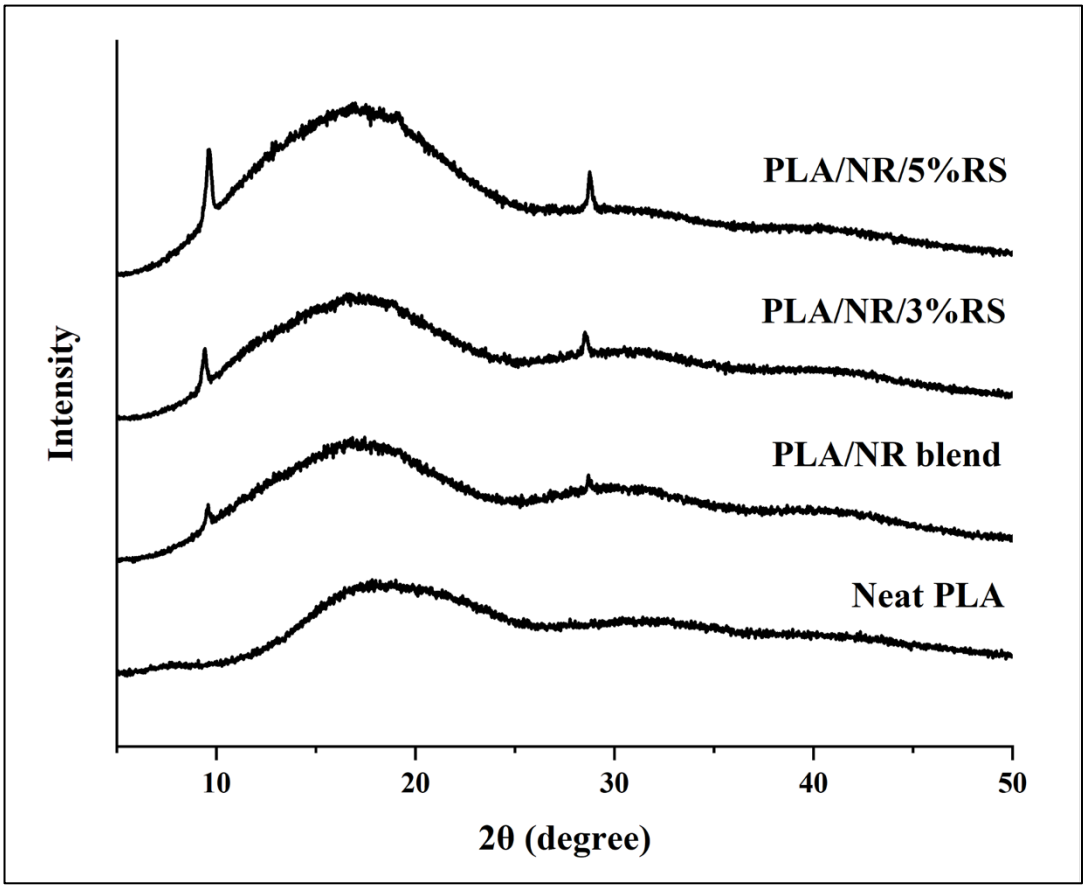

Figure 4.31 XRD patterns of film samples taken from seedling bags after growing chili plants for a period of 3 months.

4.4.2 Mulch films

In addition to their application in producing seedling bags, the neat PLA, PLA/NR blend, and PLA/NR/RS biocomposite films were employed to produce mulch films for cultivating chili plants in the field. The chili plants were cultivated for a period of 3 months, starting on April 3rd, and ending on July 3rd, 2023. Figure 4.32 presents the first day of growing chili plants, while Figures 4.33, 4.34, and 4.35 show the growth of chili plants and the physical changes that occur in the mulch films throughout periods of 1, 2, and 3 months, respectively.

Chili plants cultivated with mulch film exhibit a lower growth rate in comparison to those produced without mulch films, as seen in Figure 4.33. The use of neat PLA film as mulch resulted in the slowest growth of the chili plants. An examination of the mulch film's physical characteristics revealed that both the PLA/NR blend (d') and the PLA/NR/3%RS (e') biocomposite showed signs of cracking. Additionally, there is grass growing within the film.

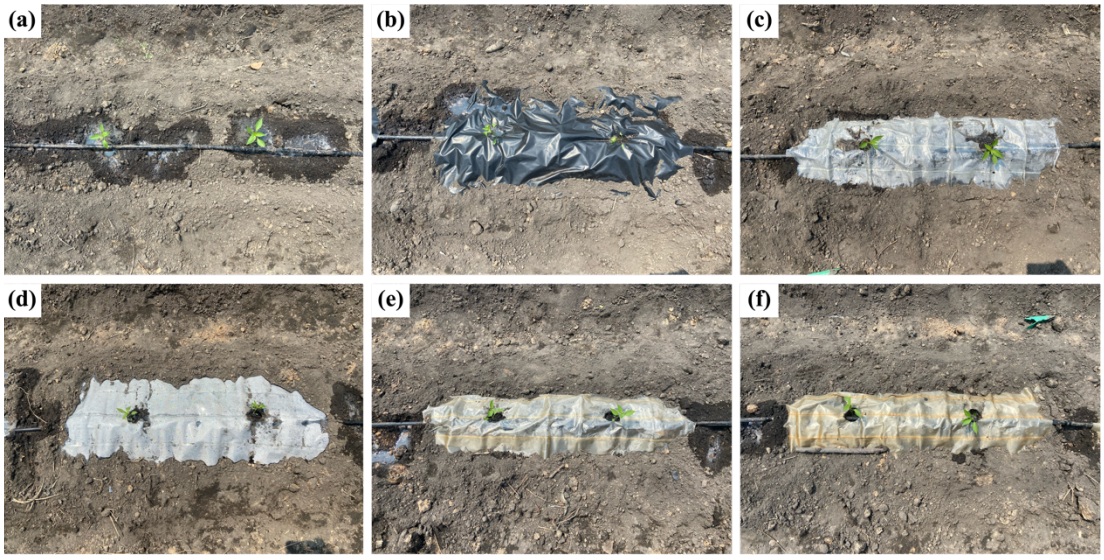

Figure 4.32 Chilli planting without mulch film (a) and with various types of mulch films: HDPE (b), neat PLA (c), PLA/NR blend (d), PLA/NR/3%RS (e), and PLA/NR/5%RS (f) biocomposite films on the first day of cultivation.

In the second month (Figure 4.34) of cultivating the chili plants, there was significant growth and production of several chili fruits. The plants cultivated with PLA mulch film grew inadequately and did not exhibit the expected growth. In addition,

it was discovered that the mulch film made from PLA/NR blend and PLA/NR/RS biocomposite film had deteriorated to the extent that it could no longer hold its initial form. Consequently, a significant amount of grass began to sprout from the cracks. Decomposition may be the cause of the mulch film's degradation.

In the final month of the chili plants' cultivation (Figure 4.35), it was observed that they had thrived and produced a huge crop of chilies. On the contrary, the chili plants that were covered with neat PLA film showed limited growth. According to Ning et al.'s (2020) report, the use of transparent film mulch increased soil temperature, resulting in a decreased growth season and decreased crop yields and quality. Furthermore, it was observed that the mulch film made from a PLA/NR blend and a PLA/NR/RS biocomposite exhibited increased degradation, leading to a failure to maintain its film form. The deteriorated film breaks into tiny pieces and disperses across the ground. A lot of grass and weeds were discovered alongside the deteriorated film tracks.

To assess the impact of mulch films on the development of chili plants, various factors, such as dry weight, stem diameter, total weight of chili fruits per plant, and height, were measured after a 3-month growing period. Additionally, the process of biodegradation of mulch films was examined after the chili planting period had finished.

Figure 4.33 Chilli planting without mulch film (a, a') and with various types of mulch films: HDPE (b, b'), neat PLA (c, c'), PLA/NR blend (d, d'), PLA/NR/3%RS (e, e'), and PLA/NR/5%RS (f, f') biocomposite films at 1 month of cultivation.

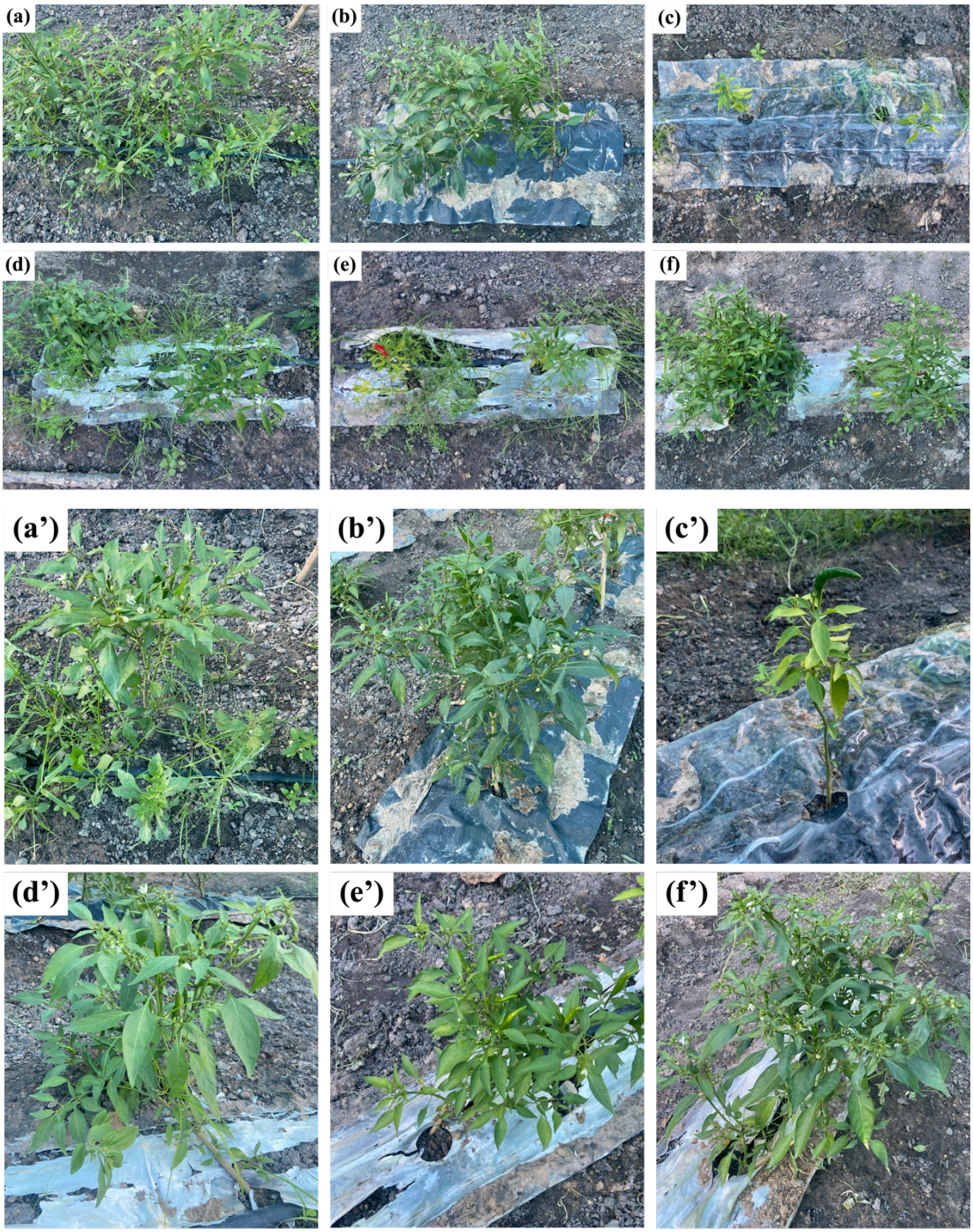

Figure 4.34 Chilli planting without mulch film (a, a') and with various types of mulch films: HDPE (b, b'), neat PLA (c, c'), PLA/NR blend (d, d'), PLA/NR/3%RS (e, e'), and PLA/NR/5%RS (f, f') biocomposite films at 2 months of cultivation.

Figure 4.35 Chilli planting without mulch film (a, a') and with various types of mulch films: HDPE (b, b'), neat PLA (c, c'), PLA/NR blend (d, d'), PLA/NR/3%RS (e, e'), and PLA/NR/5%RS (f, f') biocomposite films at 3 months of cultivation.

4.4.2.1 Dry weight, total weight of chili fruits per plant, stem diameter and height of chili plants

Figures 4.36 and 4.37 present a comparison of the dry weight, total weight of chili fruit, height, and stem diameter of chili plants grown with and without mulch films. According to the results illustrated in those figures, the growth efficiency of chili plants with mulch films made from HDPE, PLA/NR blend, and biocomposite was not significantly different. Conversely, it was discovered that chili plants grown with neat PLA mulch film had a significantly lower growth rate. The soil's exposure to high temperatures may have directly caused this. This leads to an increase in soil temperature, which has an impact on the growth of chili plants. Furthermore, the deviation range indicated that the absence of mulch film can lead to inconsistent chili plant development.

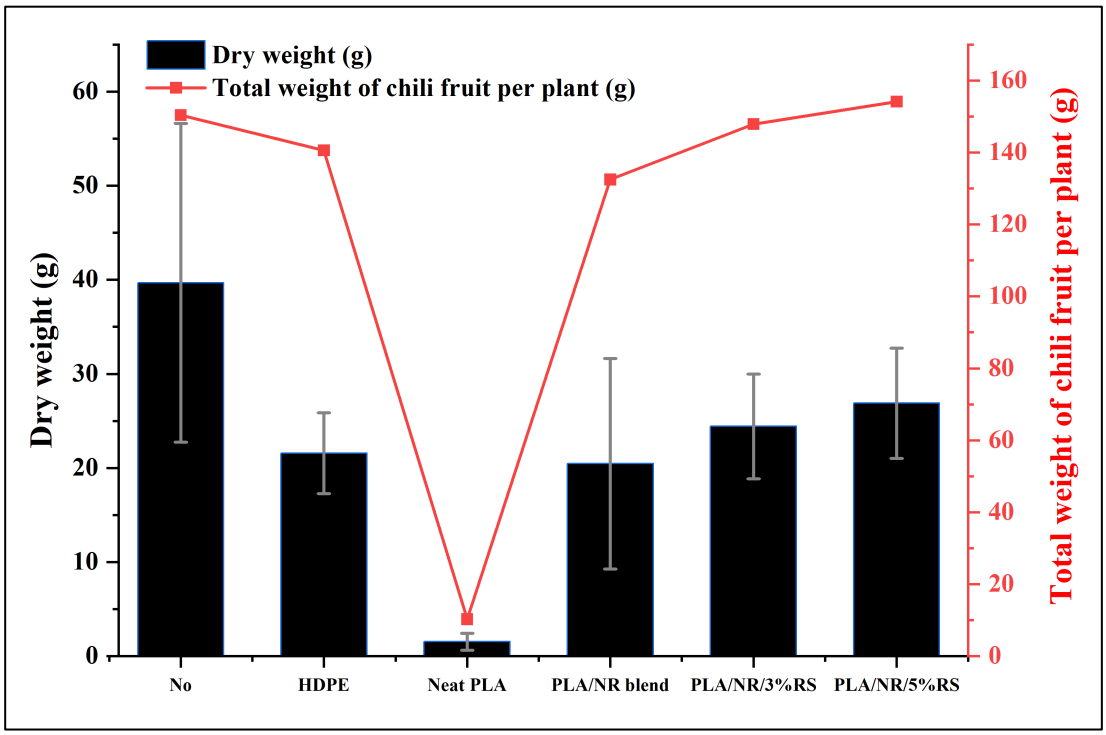

Figure 4.36 Comparison of the average dry weight and total weight of chili fruit of the chili plant grown in different types of mulch films for a period of 3 months.

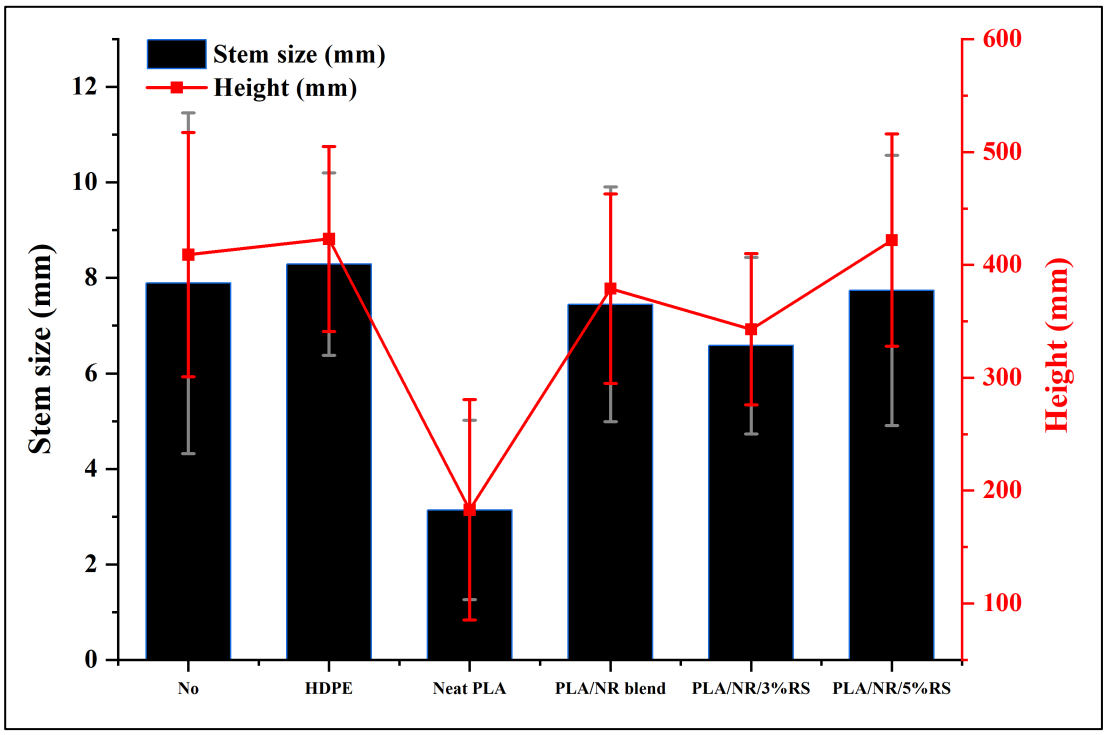

Figure 4.37 Comparison of the stem size and height of the chili plant grown in different types of mulch films for a period of 3 months.

4.4.2.2 Biodegradation of mulch films

The value for the mulch film's percentage weight loss was not available. Because of the mulch film's fragmentation and dispersion, total retrieval became impossible. This makes it impossible to obtain an accurate measurement of the percentage weight loss.

4.4.2.2.1 Molecular weight determination using GPC technique

The molecular weights of neat PLA and PLA that were extracted from PLA/NR blend and PLA/NR/ RS biocomposite film before and after being employed as seedling bags and mulch films for 90 days are shown in Table 4.9. The results from the 90-day study demonstrate a substantial decrease in the molecular weight of all films, especially those used as mulch films, due to degradation. Physical observation confirms that the mulch film breaks into tiny fragments, causing it to lose its shape, while the seedling bag remains intact. The testing of mulch films was conducted during the summer in Thailand, where the high temperatures were

approximately 40 °C. Therefore, the mulch film will be exposed to direct sunlight and heat. While the seedling bags testing was performed during the rainy season in Thailand, the seedling bag was also buried within the pots. Hence, it can be concluded that the factors important for the rapid degradation of mulch film include light and heat, through photo- or thermo-oxidative processes (Ning et al., 2020), as well as microbial degradation in the surrounding environment. Correspondence with other research that has identified UV light exposure as a significant environmental factor that affects the degradation of PLA. The study conducted by Teixeira et al. (2021) revealed that exposure to UV light has detrimental effects on the physical properties of PLA, including decreased integrity, increased brittleness, stress at break, and reduced average molecular weight.

4.4.2.2.2 Morphological properties

As shown in Figure 4.38, the FE-SEM micrographs demonstrate the surface characteristics of mulch films made from neat PLA, PLA/NR blend, and PLA/NR/RS biocomposite films after a three-month usage period. The figure indicates that the surfaces of all films exhibit roughness and lack organization, resulting from significant degradation of the surface. Additionally, compared to the surface of the seedling bags (Figure 4.29, page 87), the mulch film's surface showed large pores and a distinct separation. This signifies a higher rate of degradation. Both the film used for producing seedling bags and the mulch film used in growing chili plants are watered daily. When water and moisture from both soil and weather permeate the films, they undergo hydrolysis, leading to their degradation. Furthermore, the process of decomposition takes place because of the activity of microorganisms present in the soil. However, because of the mulch film experiment, the film is exposed to sunlight, which generates more heat than burying it like a seedling bag would. Hence, heat and light have a significant impact on the accelerated degradation of the mulch film. The results of morphological investigations of films buried in soil and films used for seedling bags and mulch film indicate that the film surface with the addition of NR and RS exhibits higher deterioration compared to the film without the addition. Therefore, it

was verified that both variables enhanced the water absorption rate of PLA, resulting in enhanced degradation.

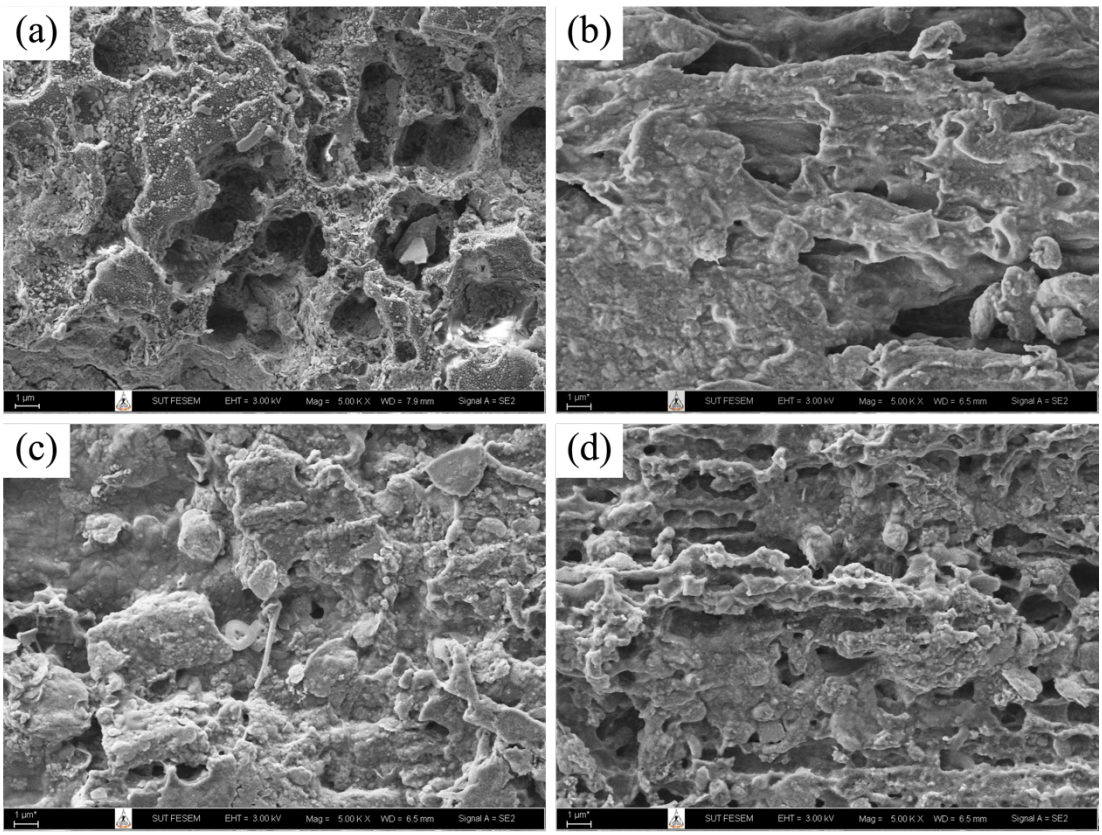

Figure 4.38 FE-SEM micrographs at 5000x magnification of mulch films produced from neat PLA (a), PLA/NR blend (b), PLA/NR/3%RS (c) and PLA/NR/5%RS (d) biocomposite films after chili planting for 3 months.

4.4.2.2.3 DSC analysis

Figure 4.39 shows the DSC thermograms obtained from film samples obtained from mulch films used for chili planting after a 3-month period. These thermograms were used for analysing changes in thermal characteristics during polymer degradation. The results of the DSC are summarized in Table 4.11. There was no significant shift in the glass transition temperature (Tg) of mulch films made from PLA/NR blend films. However, mulch films made from PLA/NR/RS biocomposite film showed a subtle change in Tg (NR) that was difficult to detect. The PLA films displayed two distinct crystal structures, as evidenced by two distinct Tm

values. The analysis revealed that the alpha’-crystal form showed a decrease in peak size, while the alpha-form crystals were larger and more visibly apparent compared to the film used for seedling bags (Figure 4.30, page 88), including the film before and after being buried in soil (Figure 4.17, page 72). This crystal form indicates a transformation in the arrangement of the crystal structure towards a more organised crystalline structure. In other hand, it was observed that both the mulch films made from the PLA/NR blend and the PLA/NR/RS biocomposite films exhibited a single crystalline form. This could be attributed to the possible interference during the chain's move to rearrangement, resulting in PLA's crystallization behavior being reduced (Devin, Ahmadi, and Taromi, 2017; Akindoyo, Beg, Ghazali, and Heim, 2018).

The Tcc of all film samples was observed to decrease. This finding is consistent with the results obtained from films used in the production of seedling bags. After conducting an analysis of the crystallinity (Xc) of the PLA phase in film samples obtained from mulch films utilised to cultivate chilli plants over a period of 3 months, it was discovered that the Xc exhibited a reduced degree of crystallinity in comparison to the film before to being buried in the soil. This happens because it is under a lot of influence, which leads to a more rapid degradation process. This includes hydrolytic, photo-, and thermo-oxidative processes, as well as the actions of different microorganisms. These factors rapidly destroy molecular chains in amorphous regions, allowing them to further attack the crystalline regions. Therefore, it is possible that the number and size of crystals may decrease.

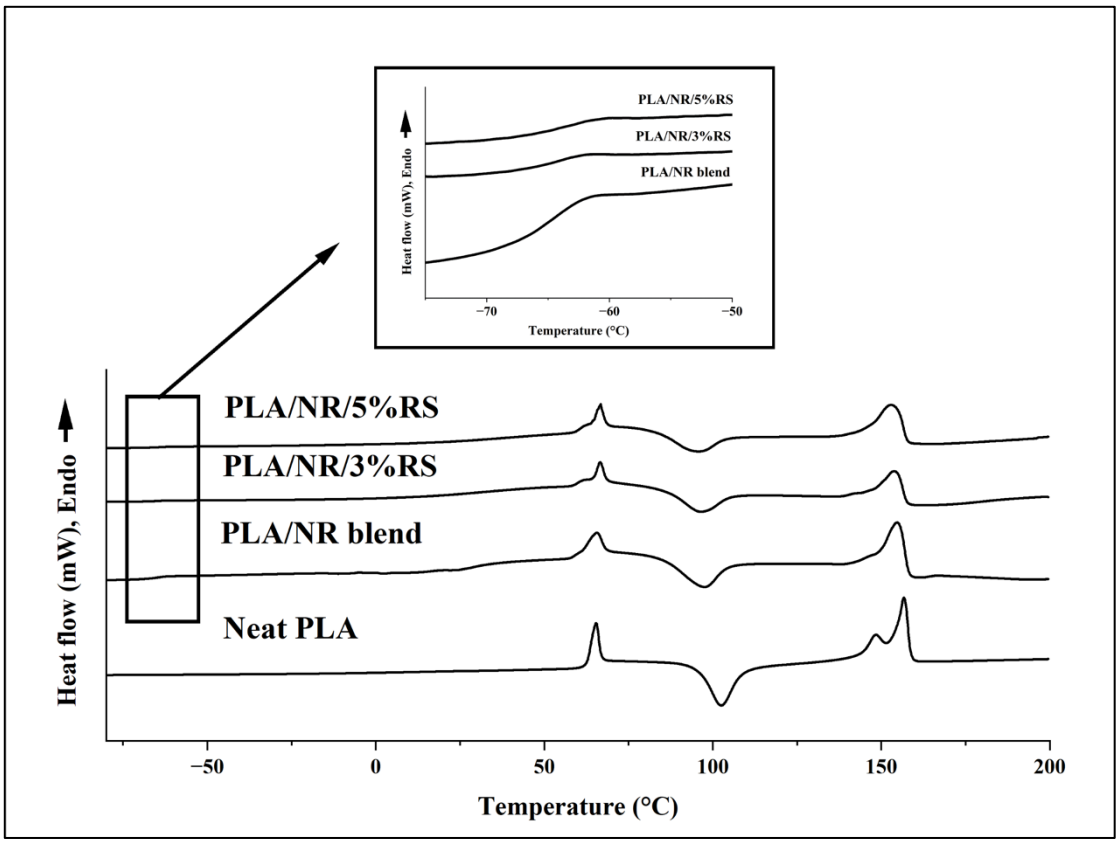

Figure 4.39 DSC thermograms of the samples taken from mulch films after growing chili plants for a period of 3 months.

4.4.2.2.1 XRD analysis

The XRD patterns displayed in Figure 4.40 demonstrate a change in the crystallinity of film samples obtained from the mulch films 3 months after planting chilli. The neat PLA exhibits a broad peak at 2θ degrees = 10° - 25°, attributed to its semicrystalline structure. The diffraction peaks of the PLA/NR blend and PLA/NR/RS biocomposite films are detected at a degree of 2θ = 10°. This investigation contrasts with the observations obtained from films that tested soil burial and used it to produce seedling bags, where diffraction peaks were discovered at 2θ degrees = 10° and 28°. In accordance with the result of a decrease in molecular weight and the results of physical observations. The mulch film had the highest rate of degradation. It is a well-known fact that PLA undergo degradation initially with its amorphous region. This results in the arrangement of the structure being more organized until the crystalline region increases. However, in this instance,

there is a decrease in crystallinity when compared to other tests, and the peak that often occurs after X-ray diffraction, caused by the refraction of atoms in the crystal sample, is absent (Ali, 2023). The decomposition of mulch film is subject to many factors, therefore increasing the possibilities of its decomposition. This decomposition can lead to the reduction in size of the crystals, making them more susceptible to water, moisture, and microbe attacks. Finally, the amount of crystalline material was decreased to a degree where it could not be detected. There is a study by Phillips, Jolley, Zhou, and Smit (2021) indicating that temperature can influence the appearance of peaks in XRD patterns. Increased temperatures can induce atomic vibrations or displacements within a crystal, resulting in a shift or broadening of the diffraction peaks. This is consistent with the utilization of outdoor mulch film, which has a long exposure to high temperatures.

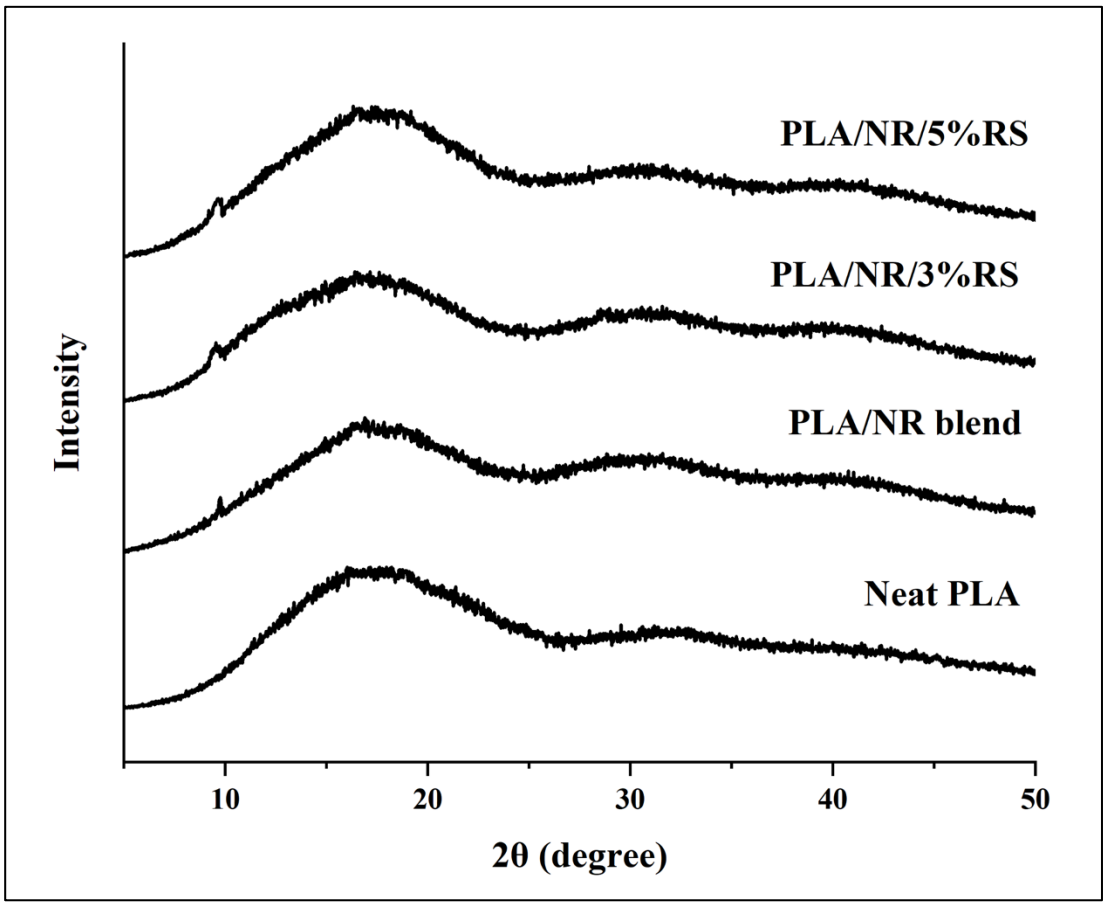

Figure 4.40 XRD patterns of film samples taken from mulch films after growing chili plants for a period of 3 months.